CRISPR-Cas effector specificity and cleavage site determine phage escape outcomes

Michael A. Schelling, Giang T. Nguyen and Dipali G. Sashital*

Roy J. Carver Department of Biochemistry, Biophysics and Molecular Biology, Iowa State

University, Ames, Iowa, USA, 50010

*Correspondence to sashital@iastate.edu

Short title: Effect of Cas12a specificity on phage escape

Abstract

1

- 2 CRISPR-mediated interference relies on complementarity between a guiding CRISPR RNA
- 3 (crRNA) and target nucleic acids to provide defense against bacteriophage. Phages escape
- 4 CRISPR-based immunity mainly through mutations in the PAM and seed regions. However,
- 5 previous specificity studies of Cas effectors, including the class 2 endonuclease Cas 12a, have
- 6 revealed a high degree of tolerance of single mismatches. The effect of this mismatch tolerance
- 7 has not been extensively studied in the context of phage defense. Here, we tested defense against
- 8 lambda phage provided by Cas12a-crRNAs containing pre-existing mismatches against the
- 9 genomic targets in phage DNA. We find that most pre-existing crRNA mismatches lead to phage
- escape, regardless of whether the mismatches ablate Cas12a cleavage in vitro. We used high-
- throughput sequencing to examine the target regions of phage genomes following CRISPR
- challenge. Mismatches at all locations in the target accelerated emergence of mutant phage,
- including mismatches that greatly slowed cleavage in vitro. Unexpectedly, our results reveal that
- 14 a pre-existing mismatch in the PAM-distal region results in selection of mutations in the PAM-
- distal region of the target. In vitro cleavage and phage competition assays show that dual PAM-
- distal mismatches are significantly more deleterious than combinations of seed and PAM-distal
- mismatches, resulting in this selection. However, similar experiments with Cas9 did not result in
- 18 emergence of PAM-distal mismatches, suggesting that cut-site location and subsequent DNA
- 19 repair may influence the location of escape mutations within target regions. Expression of
- 20 multiple mismatched crRNAs prevented new mutations from arising in multiple targeted
- 21 locations, allowing Cas 12a mismatch tolerance to provide stronger and longer-term protection.
- 22 These results demonstrate that Cas effector mismatch tolerance, existing target mismatches, and
- cleavage site strongly influence phage evolution.

25 Introduction

- 26 CRISPR-Cas (clustered regularly interspaced short palindromic repeats-CRISPR associated)
- 27 systems are adaptive immune systems found in bacteria and archaea^{1–3}. These systems use
- 28 ribonucleoprotein effector complexes to find and destroy foreign nucleic acids that have entered
- 29 the cell. CRISPR effector complexes are guided by a CRISPR RNA (crRNA) to a nucleic acid
- target that is complementary to a section of the crRNA called the spacer. Bacteria can acquire

new spacer sequences that allow them to mount an immune response against threats they have not previously encountered^{4,5}. 32 33 An important function of CRISPR-Cas systems is to prevent infection by bacteriophages, which 34 can have significant impact on the composition of a bacterial population^{6–9}. As a CRISPR 35 effector complex requires a match between its crRNA and a target to engage in interference, 36 37 selection occurs for phages with mutations in targeted genomic regions 10-12. Mutations in CRISPR targets create mismatches between the target and the crRNA that weaken the base-38 pairing interaction^{13–15}, slowing or stopping target matching by Cas effectors¹⁶ and allowing 39 phages to safely multiply in the bacterial cell. Different CRISPR-Cas systems have DNA or 40 RNA as a primary target and prevent infection at the cellular and population level 17-22. Target 41 binding is more stringent in DNA targeting systems, mitigating highly damaging off-target 42 cleavage of host DNA²³. In these systems, a protospacer adjacent motif (PAM) next to the target 43 is required to initiate base pairing²⁴⁻²⁷. Complete base pairing is especially important in the 44 region next to the PAM, called the seed region^{28–34}. Accordingly, mutations that allow phages to 45 escape CRISPR immunity are often single mutations in the PAM or seed region^{10–12,35}. 46 47 48 There have been multiple proposed but non-competing mechanisms for this mutagenesis. 49 Mutants may exist due to natural genetic variation in the population and these could be selected through CRISPR pressure and become dominant in the population over time^{11,36}. Alternatively, 50 escape mutations may be generated by Cas effector cleavage and subsequent error prone DNA 51 repair³⁷. It has been shown that cleavage by Cas effectors causes large deletions to appear in the 52 genome of T4 phage, resulting in loss of the crRNA target sequence³⁸. Lambda phage encoded 53 54 Red recombinase has been implicated in generating mutations in CRISPR targets that allow escape³⁹. It remains unclear to what degree each of these mutagenesis pathways contribute to 55 56 phage escape under different conditions. 57 58 Escape mutations are evident in natural settings as bacterial CRISPRs often contain mismatched spacers to common mobile genetic elements and the genomes of phages^{27,40–43}. New spacers are 59 added at the leader end of CRISPR arrays and these new spacers are more likely to match a 60 target in a phage genome exactly^{44,45}. Genomic evidence also shows that spacer sequences in a 61

CRISPR array do not commonly develop mutations, and are fixed once they are acquired 12,46. Instead, spacers are lost from the array entirely when they lose effectiveness as mutations 63 64 accumulate in targeted genomic elements. 65 Mismatched spacers may provide some benefit to the host. Spacers against mutated targets drive 66 67 some Cas effectors towards primed spacer acquisition, in which new spacers are preferentially acquired from genomes targeted by the Cas effector 11,31,47-50. Mismatched crRNAs may also 68 provide low level immunity through continued target cleavage. Cas effectors tolerate mismatches 69 between the crRNA and target, allowing cleavage of mutated targets^{26,28,29,51–55}. This lax 70 specificity may partially prevent phage escape. The type V-A Cas12a effector has been shown to 71 tolerate multiple mismatches between its guiding crRNA and the target in vitro^{53,56,57} leading to 72 rare off-target genome edits in cells^{57–61}. However, this mismatch tolerance varies depending on 73 74 the crRNA sequence and type of mismatch. Multiple Cas12a variants also have the ability to nick double stranded DNA targets with many (3-4) mismatches^{53,62}. These in vitro observations raise 75 76 the question of how the specificity of Cas12a affects its role in preventing infection by phage 77 with target mutations. 78 79 To test this, we subjected bacteria expressing Cas12a and crRNAs with varying target 80 mismatches to phage infection. We found unexpected discrepancies between the effect of crRNA 81 mismatches on target cleavage in vitro and survival of bacteria upon phage infection. This led us to monitor mutant emergence in phage populations. Using high-throughput sequencing, we 82 83 discovered enrichment of a large variety of mutations when the phage was targeted by different crRNAs with and without mismatches. Single crRNA mismatches, even those outside of the seed 84 85 region, had a drastic effect on the ability of bacteria to survive phage exposure, demonstrating 86 the importance of spacer diversity as mutations in target genomic regions propagate. crRNA 87 mismatches increased the rate at which mutant phage arose in the population. Mismatches in the 88 PAM-distal region led to mutations in proximity to the original mismatch, leading to highly 89 deleterious combinations of PAM-distal mismatches. Although similar mismatches were also 90 deleterious for Cas9 cleavage, similar mutants did not emerge when phage was challenged with Cas9-crRNA complexes bearing PAM-distal mutations, suggesting that PAM-distal cleavage by 91 92 Cas 12a may result in more phage escape via PAM-distal mutations. Overall, we find that phage

populations evolve in different ways to resist CRISPR interference depending on Cas effector specificity, existing crRNA-target mismatches, the location of CRISPR targets in the phage genome, and the cleavage site of the Cas effector.

Results

93

94

95

96

crRNA mismatches throughout the spacer decrease phage protection provided by Cas12a 97 98 To investigate the effect of crRNA mismatches on phage immunity provided by Cas12a, we developed a heterologous type V-A CRISPR-Cas12a system in Escherichia coli. We expressed 99 100 Cas 12a from Francisella novicida and various pre-crRNAs from two different plasmids in E. coli K12 using a strong inducible promoter (PBAD) or a relatively weak constitutive promoter^{49,63}. 101 102 We infected these cells with lambda phage to measure the immunity provided by Cas12a (Fig. 1a). We used λ_{vir} , a mutant of lambda phage that cannot engage in lysogeny and is locked into 103 104 the lytic mode of replication. This eliminates CRISPR self targeting that could occur if a target 105 phage becomes a lysogen in the bacterial genome. We chose two lambda genomic targets: one target was in an intergenic region upstream of gene J and the other target was inside the coding 106 107 region of gene L (Fig. 1a). Both genes encode essential structural tail tip proteins. The Cas12a 108 expression system exhibited a high level of protection for both promoters, with targeting crRNAs showing about 10⁶ fold less phage infection than the non-targeting control (Fig. 1b). 109 110 111 We designed 4 mutant crRNAs with varying levels of in vitro cleavage defects (Fig. 1c) and tested their effects on phage defense (Fig. 1b). These mismatches spanned the target with one in 112 113 the seed region, one in the mid-target region, and two in the PAM-distal region. We observed a 114 strong defect for the seed mutant when we used the weaker promoter to express Cas12a. 115 However, this defect was reduced upon Cas 12a overexpression using the stronger promoter (Fig. 1b), consistent with the defect being caused by reduced Cas12a targeting. Mid-target and PAM 116 117 distal mismatches caused almost no visible defects in protection for the gene J target and small 118 defects for the gene L target when Cas12a expression was controlled by the stronger promoter. 119 These results correlated with the cleavage defects measured in vitro for the corresponding mismatched crRNAs, where seed mismatches had stronger defects than other mismatches but 120 still enabled complete cleavage (Fig. 1c, S1 Fig.), consistent with previous results^{53,54}. However, 121

when Cas12a expression was controlled by the weaker promoter, we observed a large loss of protection for the mid-target mismatched cRNA targeting gene J, which had no significant loss of cleavage in our in vitro assay (Fig. 1b,c, S1 Fig.). These results suggest that factors outside of reduced targeting may affect Cas12a-mediated protection at low expression levels.

We then tested the effects of mismatched crRNAs in liquid culture when Cas12a was expressed from the stronger promoter. Cells containing a matching crRNA grew at the same rate as cells that were uninfected with phage, demonstrating complete Cas12a protection in the time frame tested (Fig. 1d). In contrast, most mismatched crRNAs caused lysis to occur regardless of the mismatch location in the target. For the gene J target, a crRNA mismatch in the seed region caused lysis to begin 1 h after infection, similar to a culture bearing a non-targeting crRNA. This indicated that the seed mismatch was allowing nearly full phage escape, consistent with this mismatch causing the largest reduction of target cleavage in vitro (Fig. 1c).

In contrast, the seed mismatched crRNA against gene L provided protection for several hours post infection, with lysis beginning 3 h post-infection (Fig. 1d). Mismatches in the mid- or PAM distal region offered protection until four or five hours following infection. Interestingly, the rate of cleavage for these crRNAs did not always correlate with the level of protection provided in liquid culture (Fig. 1c-d). Some crRNA mismatches that caused small decreases or no significant effect on cleavage rates in vitro led to lysis of the culture (e.g. gene J position 8 and gene L position 15). These results indicate that loss of cleavage caused by crRNA mismatches did not completely account for loss of immunity.

Phage target mutations depend on location of existing mismatches

Our initial results showed that crRNA mismatches have less of an effect on solid media than in liquid culture when Cas12a is expressed from a strong promoter. We hypothesized that these differences were caused by phage mutation upon CRISPR immune pressure. Unlike on solid medium, phage mutants that arise can quickly and uniformly spread throughout the culture in a liquid medium. Thus, pre-existing mismatches or mismatches that arise through imperfect DNA repair following Cas12a cleavage may accelerate the selection for escape mutants as they quickly

spread throughout the population, causing lysis in liquid culture. These results overall suggested that loss of protection from crRNA mismatches is due in part to emergence of phage mutants that further disable CRISPR interference. To test this hypothesis, we investigated mutations that arose in phage populations in response to CRISPR pressure by Cas12a effector complexes with or without pre-existing crRNA mismatches (Fig. 2a). We isolated phage from liquid cultures of E. coli expressing matching or mismatched crRNAs and PCR amplified the regions of the phage genome that were being targeted. Highthroughput sequencing was then used to identify mutations in the target regions. We first quantified the percent of the phage population that had mutations in genomic regions targeted by Cas12a over time in liquid culture. We observed mutations within the targeted region of PCR amplicon sequences, but not outside of the target region. Phages targeted by a matching crRNA gradually developed target mutations over time, with about 20% of the phage population becoming mutated after the 8 hour time course (Fig. 2b). A crRNA mismatch at any of the positions we tested led to a large acceleration of mutant emergence causing the phage population to become almost entirely mutated after 4 hours. Interestingly, phages exposed to bacteria expressing crRNAs with a seed mismatch also rapidly mutated, even though our in vitro results showed the original crRNA mismatches were highly deleterious for target cleavage (Fig. 1c). For most individual replicates of our samples, we did not observe substantial variability in the distribution of mutations after the phage population became highly mutated (S2a Fig.). We therefore chose to focus on the longest time point (8 h) for further analysis. As previously shown in other CRISPR systems 10,35,64, phage populations targeted with a perfectly matching crRNA developed mutations in the seed region of the target (Fig. 2c). When the sequences of the crRNA plasmids were changed to create mismatches between the crRNA and the phage genome target, the position of individual point mutations within the phage target became substantially more variable. A crRNA mismatch at position 3 for the crRNA targeting the region upstream of gene J caused 9 different individual point mutations to appear at 8 positions spread across the PAM and seed, none at position 3 as expected given the pre-existing mismatch (Fig. 2c). For the gene L target, a crRNA mismatch at position 3 only caused 2

152

153

154

155

156157

158

159

160

161

162

163

164

165

166

167

168

169

170

171

172

173

174

175

176

177

178

179

180

different mutations to appear, with one of them being the predominant mutation seen when targeting with a matching crRNA. Mismatches in the mid-target region at position 8 also caused seed mutations to arise. Surprisingly, PAM-distal crRNA mismatches caused enrichment of PAM-distal mutations and prevented nearly all seed mutations from emerging. Most of the mutations present in liquid culture were also observed when sequencing phage from spot assays, although the distribution differed in some cases (S2b Fig.). This indicates that the differences we observed between our solid media and liquid cultures experiments were caused by the increased mobility of phages in liquid culture, and were unrelated to the types and location of mutations that could arise.

The genomic context of target sequences had a clear effect on the types of mutants that emerged (Fig. 2d, S2c Fig.). For the matching crRNA targeting the region upstream of gene J, the most common mutation observed was a single nucleotide deletion at position 6. The most common mutation for the gene L target was a single nucleotide substitution at position 2 which is a wobble base position in the codon. Similar to the other mismatched crRNA constructs targeting gene L, most mutations we observed were either silent or caused amino acid changes from valine, threonine or serine to alanine or from proline to leucine. No deletions were observed in the gene L target in any samples with crRNA mismatches, while deletions were observed in the gene J upstream target in samples with crRNA mismatches at positions 15 and 19. This difference in mutational variability reflects the more vulnerable target region of gene L where base substitutions are likely to change the amino acid sequence of the protein and single deletions will cause frame-shifts. The relatively weak constraints on viable mutations in the upstream region of gene J may enable more routes for escape from Cas12a targeting, resulting in the loss of protection at earlier time points (Fig. 1d).

Phage mutations can arise following exposure to Cas12a

Our results indicate that mutations can arise rapidly in regions targeted by Cas12a when a preexisting mismatch is present between the crRNA and target. It is possible that Cas12a targeting selects mutant phages that are present in the population at the time of infection. We investigated whether the mutated phage we observed in our CRISPR active samples were present in negative control samples. While many of the single-nucleotide substitutions that were enriched following Cas 12a targeting were present at very low levels in the control sample, we could not distinguish actual nucleotide variations from sequencing or PCR error (S3 Fig.). However, we did observe that two out of three sequences containing single-nucleotide deletions that were consistently present in control samples were the only two deletion mutants that became highly enriched in the escaped mutant phage population (S2c Fig., S4 Fig.). These results suggest that deletion mutants that were enriched upon Cas12a-mediated selection were pre-existing in the population. To further test this, we designed crRNAs targeting non-essential regions in the lambda phage genome (S5 Fig.). Cas12a-mediated defense against lambda phage using these crRNAs caused large deletions to appear based on recombination at microhomology sites, as has been previously observed³⁸ (S5a,b Fig.). We used long-read sequencing to determine whether these regions of the wild-type lambda phage population contained the same deletions. Similar to the singlenucleotide deletions, microhomology-mediated deletions that were enriched upon Cas12amediated selection were among the most abundant mutations pre-existing in the wild-type population (S5c Fig.). Together, these results suggest that mutants that emerge upon Cas12a targeting may be selected from natural genetic variants in the population. Our observation that enriched deletion mutations pre-exist in the wild-type population does not rule out the possibility that mutations may be actively acquired following Cas12a cleavage. Previous studies have suggested that DNA cleavage by Cas9 or Cas12a may induce mutation in the target site through DNA repair^{35,38}. To test this possibility, we deleted the *red* operon from the λ_{vir} genome, which has previously been implicated in escape mutation enrichment following targeting by Cas 9^{39} . We performed liquid culture infection assays using the Δred phage in cultures expressing Cas12a and panel of crRNAs described above (S6a Fig.). Unlike with wildtype phage, infection with the Δred phage did not cause lysis in most cultures expressing a perfect or mismatched crRNA. We next sequenced phage populations harvested from cultures 8 hr after infection (Fig. 2c, S6b Fig.). Consistent with the lack of lysis in many cultures, we did not observe mutants arising in cultures expressing either perfect crRNA, the PAM-distal mismatched crRNAs targeting gene J, nor the mid-target mismatched crRNA targeting gene L. For most of the remaining crRNAs, we

214

215

216

217

218

219

220

221

222

223

224

225

226

227

228

229

230

231

232

233

234

235

236

237

238

239

240

241

242

243

observed mutations that were observed in the wild-type phage populations challenged with the same crRNA, although the number of mutants and distribution of these mutants varied between phage strains. One notable exception where we observed new mutations arising in the Δred strain was for the phage challenged with the mid-target (position 8) mismatched crRNA targeting gene J (Fig. 2c). Surprisingly, we observed a range of double mutations in the mid and PAM-distal region in Δred phage challenged with this crRNA (Fig. 2c, S6b,c Fig.). Importantly, all double mutants observed in individual replicates contained unique mutations and appeared to originate with a single point mutation (S6c Fig.). These results strongly suggest an active mechanism of mutant generation unrelated to the red operon. Overall, our results provide evidence that both preexisting and actively acquired mutations may be selected during Cas12a-mediated immunity. Multiple mismatches in the PAM distal region allow phage escape from Cas12a A striking result from our sequencing of mutant phage populations was the emergence of PAMdistal mutants upon challenge with crRNAs containing PAM-distal mismatches. Given that seed mutants appeared when other Cas12a crRNAs were used, these results suggested that multiple PAM-distal mismatches are at least as deleterious for Cas12a cleavage as a seed mismatch combined with a PAM-distal mismatch. It has been shown that pairs of mismatches are more deleterious for Cas12a cleavage when they are closer together, including when both are in the PAM-distal region^{53,56}. Together, these results suggest that double mismatches in the PAM-distal region can lead to phage escape from Cas12a. To test this, we added second PAM-distal crRNA mismatches to crRNAs targeting gene J that initially contained a single PAM-distal mismatch. We chose the second mismatch position based on phage mutants that appeared when exposed to the original mismatched crRNA (Fig. 2d, S7a Fig.). Adding a second mismatch at position 14 to the crRNA that contained a mismatch at position 15 caused a small defect in phage protection (Fig. 3a). Although this mismatch pair had small effects on the overall cleavage rate in vitro regardless of the mismatch type at position 14 (Fig. 3b, S7b-c Fig.), we did observe a cleavage defect, in which the DNA was nicked by Cas12a through cleavage of only one strand (S7b Fig.). This defect in second-strand cleavage may allow

245

246

247

248

249

250

251

252

253

254

255

256

257

258

259

260

261

262

263

264

265

266

267

268

269

270

271

272

273

more phage infection, resulting in partial loss of phage defense on solid media (Fig. 3a). 275 276 Consistently, bacteria expressing a crRNA with a position 15 mismatch did not lyse in liquid 277 culture (Fig. 1d), despite the emergence of the position 14 mutation (Fig. 2c-d). In contrast, adding any type of second mismatch at position 16 to a crRNA that contained the original 278 279 mismatch at position 19 caused nearly complete loss of protection (Fig. 3a) consistent with lysis 280 observed for the position 19 mismatched crRNA in liquid culture (Fig. 1d) and the dramatic loss 281 of cleavage activity in vitro (Fig. 3b, S7b-c Fig.). 282 283 We next investigated why PAM-distal mutations may be preferentially selected over PAM or 284 seed mutations that may be highly deleterious to Cas 12a cleavage on their own. Notably, while PAM and seed mutations were not highly enriched for wild-type phage challenged with PAM-285 286 distal mismatched crRNAs in liquid culture (Fig. 2c), we did observe PAM and seed mutants when we assayed the phage population present in spot assays on solid media (S2b Fig.). This 287 288 difference may be due to competition between different mutant phages, in which phages bearing 289 mutations that are more deleterious to Cas12a cleavage may outcompete less deleterious 290 mutants. Such competition is more likely to occur in liquid media where phages are mobile. 291 292 To test this hypothesis, we isolated two mutant phages selected upon targeting with the position 293 15 mismatched crRNA (MM15) targeting gene L (see Methods). The mutant phages contained a 294 single point mutation in either the seed (A2T) or the PAM-distal region (G17T) of the gene L 295 target region. As expected, the seed mutant phage caused a far greater loss of protection than the 296 PAM-distal mutant when the two mutant phages were used to infect bacteria expressing Cas12a and the perfectly matching crRNA in phage spotting assays (Fig. 3c). In contrast, both mutants 297 298 caused a similar loss of protection in cells expressing the MM15 crRNA. 299 300 We next tested the extent to which these target mutations cause Cas 12a cleavage defects using 301 both the perfect crRNA and the MM15 crRNA (Fig. 3d, S8 Fig.). Cleavage of the A2T seed 302 mutant target was reduced by 15-20x in comparison to the WT target, and we did not observe a 303 significant difference in cleavage of this target by Cas12a bearing either the perfect or MM15 crRNA (Fig. 3d). Strikingly, Cas12a cleavage was reduced by ~90x when the G17T target was 304 305 cleaved with Cas12a bearing the MM15 crRNA. Importantly, this loss of cleavage upon

306 introduction of two PAM-distal mismatches was significantly more deleterious than the cleavage 307 defect observed when seed and PAM-distal mismatches were combined (MM15/A2T 308 combination). 309 Together, our results strongly suggest that PAM-distal mutants emerge upon challenge with 310 311 crRNAs bearing PAM-distal mismatches because two PAM-distal mismatches can be more 312 deleterious to Cas12a cleavage than a seed and a PAM-distal mismatch. To directly test this, we 313 performed a competition assay in liquid culture in which cells expressing either a non-targeting 314 or the MM15 crRNA were co-infected with a mixture of the A2T and G17T mutant phages (Fig. 3e-f). We performed the competition at decreasing phage concentrations, allowing competition 315 to occur as the phages were propagated in the culture. Lysates were sampled after 8 hr, the target 316 317 region was PCR amplified, and the abundance of each mutant was determined by highthroughput sequencing. 318 319 Notably, although both the A2T and G17T substitutions are silent mutations, the A2T mutant 320 321 slightly outcompeted the G17T mutant in cultures expressing the non-targeting crRNA (Fig. 3f), suggesting that the A2T mutant phage may be slightly more fit than the G17T mutant. In 322 323 contrast, when co-infection was performed in cultures expressing the MM15 crRNA, the G17T 324 mutant became dominant in the phage population when cultures were infected with highly 325 diluted phage mixtures. Overall, our results demonstrate that PAM-distal mutants emerge in liquid cultures expressing PAM-distal mismatched crRNA because of the highly deleterious 326 327 effect of dual-PAM distal mismatches on Cas12a cleavage. 328 329 330 Emergence of PAM-distal escape mutants occurs for Cas12a but not Cas9 Our results show that some pairs of PAM-distal mismatches are deleterious enough to cause 331 escape from CRISPR-Cas12a immunity. We also note that Cas12a cleaves in the PAM-distal 332 region of the target²⁶, and that our and previous results suggest that mutations may arise during 333 repair of DNA breaks induced by Cas endonuclease cleavage^{38,39}. Thus, it is possible that Cas 12a 334 is uniquely prone to emergence of escape mutations in the PAM-distal region. 335

To test this hypothesis, we performed similar experiments for *Streptococcus pyogenes* Cas9 (SpCas9), which cleaves targets in the PAM-proximal region^{55,65} and therefore may be more prone to emergence of mutations in the PAM and seed region. Similar to FnCas12a, in vitro cleavage assays using SpCas9 revealed that two PAM-distal mismatches cause a significantly larger defect than a seed and PAM-distal mismatch (Fig. 4a). Surprisingly, for the target tested in our in vitro cleavage assays, the PAM-distal mutation was more deleterious than the seed mutation even when targeted by the perfect crRNA. These results suggest that PAM-distal mutations should be sufficient to cause escape from SpCas9-mediated immunity.

To test whether such mutants emerge, we performed liquid culture phage challenge assays in *E. coli* expressing SpCas9 programmed with single guide RNA (sgRNA) containing mismatches at the same positions relative to the PAM as those tested for FnCas12a (Fig. 4b, S10a Fig.). Similar to FnCas12a, mismatches caused minimal defects in SpCas9-mediated phage defense on solid media (S10a Fig.). In liquid media, delayed lysis occurred in all cultures, including those expressing perfect crRNAs (Fig. 4b). To determine whether lysis occurred due to the emergence of phage mutants, we PCR amplified the target regions of phage collected from these lysates and sequenced the amplicons by high-throughput sequencing. Mutants emerged in all samples and target mutations were confined to the PAM and seed, although the positions of these mutations varied (Fig. 4c, S10b Fig.). Seed and mid-target crRNA mismatches caused a shift away from the PAM and into the seed region. Unlike Cas12a, no PAM-distal mutants emerged for either target when challenged by Cas9 bearing PAM-distal mismatched sgRNAs. These results suggest that both Cas effector specificity and cut site may impact the location within targets at which escape mutations may emerge.

Phage targeted with mismatched spacers develop conditional escape mutations

Our results suggest that individual mismatches are often not sufficiently deleterious to allow phages to escape Cas12a targeting. Instead, the combination of the pre-existing mismatch and an additional mutation in the target is necessary for escape to occur. It remains unclear to what extent these new mutations contribute to phage escape in the presence of a pre-existing mismatch. We chose to pursue further experiments using the crRNA with a seed mismatch targeting gene J because although it was highly deleterious for cleavage in vitro (Fig. 1c), it

caused rapid phage mutation in liquid culture (Fig. 2b). In addition, this mismatch caused the largest variety of mutants to arise for all the crRNAs we tested with mutations at nearly all positions in the seed region (Fig. 2c, S2 Fig.). We hypothesized that this target in an intergenic region was less restrictive of mutation, exacerbating the defect of this crRNA mismatch in vivo. To test this hypothesis, we generated mutated phage populations using the seed mismatched crRNA targeting gene J. We first infected E. coli cells expressing the mismatched crRNA with lambda phage in liquid culture at a wide range of MOIs (Fig. 5a). The phages were able to clear the culture at MOIs greater than 1.5×10^{-3} (S11a Fig.). We then analyzed the genomic diversity of the phage population in the targeted region using high-throughput sequencing. The phage population retained the wild-type sequence of the target region at the two highest MOIs tested (0.15 and 0.075 MOI), indicating that the wild-type phage can overcome Cas12a-mediated immunity when the bacteria are exposed to enough phage particles (Fig. 5b). At the lowest MOIs tested, 1.5 x 10⁻⁴ and 1.5 x 10⁻⁵, 99% of the phage population contained a single mutation at the first position of the protospacer. Mutations that arose were most varied at intermediate MOIs. These mutations were in the seed region or mid target region near the existing crRNA mismatch. The number of different mutations observed was also higher compared to the bacterial strain with a matching crRNA to the WT phage target. Next, we harvested phage from the cultures at all of the MOIs tested and compared protection against this mutant phage population by a crRNA that perfectly matched the wild-type target and a crRNA bearing the original seed mismatch used to generate the mutant population. Visible infection using these new phage lysates was first observed when using phage that was 48% mutated (Fig. 5c, S11b Fig.). While the perfect crRNA still offered some level of protection against the mutated phage, the crRNA containing the mismatch resulted in complete loss of protection (Fig. 5d-e). These results indicate that some mutations that emerge in the phage population are only significantly deleterious to Cas12a interference in the presence of the preexisting mismatch, revealing the importance of combined mismatches for phage escape.

367

368

369

370

371

372

373

374

375

376

377

378

379

380

381

382

383

384

385

386

387

388

389

390

391

392

393

Combining mismatched spacers increases level of protection

395

396

397

398

399

400

401

402

403

404

405

406

407

408

409

410

411

412

413

414

415

416

417

418

419

420

421

422

423

424

425

Our results indicated that loss of protection by Cas12a due to crRNA mismatches was only partially caused by loss of Cas12a cleavage due to the pre-existing mismatch, and that mutant emergence generating a second mismatch also contributed substantially to this loss of protection. These results imply that Cas12a mismatch tolerance should enable stronger and longer term protection under conditions where phage mutants are less likely to emerge. To further test this, we introduced both the gene J and L crRNAs into a CRISPR array for co-expression of both crRNAs (Fig. 6a). It has been demonstrated previously that bacterial populations with diverse spacer content in their CRISPR arrays show robust immunity against phage at the population level as phage are unable to develop escape mutations in all of their targeted genomic regions^{66,67}. Cas 12a expressed along with multiple different cRNAs shows increased phage resistance compared to when a single crRNA is present, but the mechanism of this increased resistance is not clear⁶⁴. We investigated this mechanism further in the context of our previous experiments with mismatched crRNAs. If the loss of protection due to a crRNA mismatch is caused only by a slowing of the rate of cleavage, then two different mismatched spacers should not provide more protection than one spacer repeated twice. Alternatively, if phage mutant emergence significantly contributes to loss of protection in the presence of a crRNA mismatch, two different mismatched spacers should provide better protection than a single mismatched spacer repeated twice. Consistent with the second possibility, the CRISPR construct with two unique mismatched spacers (hereafter referred to as double spacer construct) showed a significantly higher level of protection than either of the crRNA constructs with two copies of a single mismatched spacer (hereafter referred to as single spacer construct) when measured by plaque assay (Fig. 6b). Similar to liquid cultures with bacteria expressing a single copy of the crRNA, we observed faster lysis of the gene J targeting crRNA in comparison to the gene L targeting crRNA, consistent with the higher chance of escape mutant emergence against the gene J crRNA. Bacteria expressing the double spacer construct showed slowed growth between 1 and 2 hours but recovered quickly and did not lyse over the time course tested (Fig. 6c). Phage from these cultures was harvested over time and used to infect CRISPR inactive bacteria to determine the relative titers. Phage titers decreased over time in cultures expressing the double spacer

construct, while the phage titer increased over time in cultures with cells expressing the single spacer constructs (Fig. 6d).

Spotting these same phage lysates on CRISPR active cells showed no noticeable infection by lysate harvested from the double spacer culture, but moderate infection by the single spacer lysate (S12a Fig.), suggesting that escape mutants did not emerge from bacteria expressing two different mismatched crRNAs. Consistently, sequencing of both target regions in individual plaques revealed mutations in only one of the two target regions (Fig. 6e, S12b Fig.). Together with our previous results, these results suggest that loss of protection due to a crRNA mismatch is caused by a combination of loss of Cas12a targeting and the emergence of mutant phages that further block CRISPR interference.

Pre-existing target mutations cause different CRISPR escape outcomes

We have shown that target mismatches artificially introduced by changing crRNA sequences accelerate phage escape and increase the diversity of mutations that appear. We wanted to determine if the same effect would appear if the crRNA-target mismatch was instead caused by a phage genome mutation. We first generated clonal phage populations with single target mutations by isolating individual plaques of mutant phage that emerged following exposure to Cas12a bearing various crRNAs (Fig. 7a). Using a crRNA containing a seed mismatch, we isolated phages with mutations in the PAM (T-2C) or seed (C2A) (S13a,b Fig.), while a crRNA containing a mismatch at position 19 allowed us to isolate two separate plaques containing phage with a mutation at position 16 (G16T) (S13c,d Fig.). After propagating phage from these plaques, we challenged the mutant phages to CRISPR pressure by bacteria expressing crRNAs with a spacer matching the wild-type phage genome target. We observed that the phage with a seed region mutation caused rapid lysis of CRISPR active bacteria (Fig. 7b). This indicated that the C2A mutation was a complete escape mutation. However, phage mutations in the PAM or PAM-distal region caused delayed lysis to occur. In particular, of the two G16T isolates, only one caused lysis to occur in some of the experimental replicates (Fig. 7b).

We harvested phage from the previous cultures and sequenced PCR amplicons of the phage genome targets using Sanger sequencing. In the seed mutant (C2A) phage cultures, the phage

retained the same seed mutation and did not develop additional mutations (Fig. 7c, S13b Fig.), further indicating that C2A is a bona fide escape mutation on its own. In phage with pre-existing mutations in the PAM, mutations appeared at the edge of the seed region (Fig. 7c, S13a Fig.). In phage with a pre-existing mutation in the PAM-distal region at position 16, mutations appeared at positions 14 or 18 for phage harvested from cultures that lysed. Repeating the same experiment with PAM-distal mutants in the gene L target similarly caused further mutations to occur in the mid-target and PAM-distal regions (S13e-h Fig.). We proceeded with further experiments using only replicates in which a clonal phage population was generated based on an unambiguous Sanger sequencing chromatogram (S13a,b,d Fig.). Using these phage, we sought to verify that these second mutations were allowing CRISPR escape. We compared infection of bacteria expressing the matching crRNA by purified phage containing a single target mutation and phage with two target mutations. As expected, phage with the seed target mutation infected bacteria expressing the perfect crRNA at the same level as bacteria expressing a non-targeting crRNA (Fig. 7d). Phage with single target mutations in the PAM or PAM distal region infected bacteria expressing the perfect crRNA at a level close to wild-type phage, while phage with a second mutation infected 10⁴ to 10⁵ times more (Fig. 7d). We conclude that target mutations that do not lead to significant CRISPR escape can accelerate the appearance of second mutations that allow complete escape. **Discussion** In order for Cas12a to be an effective immune effector, it must provide immunity from bacteriophage in diverse conditions. The physical environment controls which bacteria are

456

457

458

459

460

461

462

463

464

465

466

467

468

469

470

471

472

473

474

475

476

477

478

479

480

481

482

483

484

bacteriophage in diverse conditions. The physical environment controls which bacteria are exposed to which phages, and the dispersal of new phage particles after infection and lysis^{9,68}. We found that Cas12a overall provided more robust immunity on solid media than in liquid culture. The effect of seed crRNA mismatches using either media correlated with the deleterious effect of the crRNA mismatch on rate of cleavage in vitro. Mid-target and PAM-distal mismatches, however, showed a much more drastic effect in liquid culture than defects observed in vitro or on solid media when Cas12a was expressed from a strong promoter, causing eventual lysis of the bacterial population, sometimes at a rate similar to seed mismatches. These results

strongly indicate that the effect of crRNA mismatches varies depending on the environment where phage exposure may occur.

Although phage can escape CRISPR interference with a single mutation in the seed region ^{10,35}, our results indicate that a seed mutant is sometimes not deleterious enough to allow complete escape. Instead, the mechanism of phage escape occurs through the emergence of mutations that further weaken CRISPR interference when a mismatch is present. This is supported by the rapid emergence of mutant phage we observed even when a highly deleterious seed crRNA mismatch was present. In addition, the number of different mutations that appeared increased when a crRNA mismatch was present, and the distribution of these mutations greatly varied depending on the location of the mismatch. These results suggest that mismatches between the crRNA and target decrease phage protection by broadening the range of mutations that allow escape. This mechanism also explains the deleterious effect of mismatches at some positions outside of the seed region on immunity in liquid culture that does not appear during in vitro cleavage.

In natural settings, spacer-target mismatches are caused by phage genome mutation rather than CRISPR spacer mutation that would change the sequence of the crRNA^{12,69}. Phages with a single target mutation might not be able to completely escape from certain CRISPR spacers, requiring selection of a second target mutation for full evasion of CRISPR interference³⁶. This scenario may become more likely if the seed region, where mutations would normally arise, is located in a critical part of the genome where mutations are highly deleterious. Supporting this, we isolated phage with single mutations in both intergenic (gene J) and coding (gene L) regions that did not cause significant CRISPR escape that then developed second mutations that allowed full escape when exposed to the matching crRNA. In addition, CRISPR spacers with multiple mismatches become more abundant over time in natural populations⁴⁶. Thus, the presence of mutations may drive further mutation in CRISPR targets over time.

When a PAM-distal crRNA mismatch or a PAM-distal target mutation was present, mutations arose in close proximity to the pre-existing mismatch for Cas12a, but not for Cas9. Our in vitro cleavage results suggest that two PAM-distal mismatches may be more deleterious than individual seed mismatches, or even combinations of seed and PAM-distal mismatches. Thus,

phage mutations that result in multiple PAM-distal mismatches are more likely to be selected than PAM or seed mutants when a PAM-distal mismatch already exists.

The enrichment of PAM-distal mutations after exposure to Cas12a and not Cas9 may be influenced by their cut sites, which are in the PAM-distal region and downstream of the target for Cas12a and in the seed region for Cas9^{26,55,65}. Mutations may be more likely to arise around the cleavage site due to DNA repair that occurs after cleavage by Cas12a or Cas9. Notably, many of the crRNAs used in our study caused initial nicking, rather than complete double-strand cleavage, in in vitro cleavage assays (S1b Fig., S7b Fig., S8b Fig., S9b Fig.). Such nicking events may result in recombination or other DNA repair mechanisms that result in alteration of the sequence around the cleavage site. Indeed, there is evidence that phage escape mutation is accelerated by error prone repair after cleavage by Cas effectors and mediated by phage recombinases, especially when a crRNA provides a low level of protection^{38,39}. Lambda phage

recombination enzymes in particular have been shown to increase the appearance of mutated phage in populations under CRISPR pressure³⁹. Our results suggest that some mutants that arose upon Cas12a challenge pre-existed in the population, especially for mutants involving single nucleotide or long deletions. However, we also observed strong evidence that mutants arose following Cas effector targeting, including in phage strains lacking Red recombination machinery. We speculate that pre-existing mutations may be propagated in the phage population by lambda encoded recombinases, but that error prone repair following Cas effector cleavage is not dependent on Red recombination. Phage with target mutations in their genome that initially survive interference could be used as recombination substrates to pass along that mutation to

Overall, our results reveal that mismatches throughout the crRNA-target duplex can drastically decrease protection provided by Cas12a. However, there are fundamental differences between our heterologous system and natural CRISPR-Cas systems. Adaptation is an important part of CRISPR immunity. As phage mutate and become immune to targeting by existing spacers, new spacers from the phage genome can be added to the CRISPR array^{11,70}. It remains to be

other phages in the cell. This could account for the rapid increase in mutant phages we observe

and the deleterious effect of phage recombination enzyme knockouts³⁹.

investigated how mismatched spacers contribute to acquisition of new spacers in type V systems, 546 especially using a primed mechanism as occurs in type I and type II systems. 547 **Materials and Methods** 548 **Expression plasmid construction** 549 550 All primers and plasmids used in this study are listed in S1 Table. Cas12a and Cas9 expression 551 plasmids were constructed using pACYCDuet-1. A gene expressing FnCas12a or SpCas9 was inserted downstream of a pBAD promoter in pACYCDuet-1 using Gibson assembly. Promoters 552 were replaced with a previously described low copy P4 promoter⁴⁹ using one piece Gibson 553 554 assembly, crRNA expression plasmids were constructed using pUC19. A pBAD promoter was inserted into pUC19 in the multiple cloning site with Gibson assembly. "Round the horn" PCR 555 556 and ligation was used to add a mini CRISPR array with one or two spacers downstream of the 557 pBAD promoter. The same method was used to replace mini CRISPR arrays with Cas9 sgRNA 558 expression constructs. 559 560 **Bacterial and phage strains** E. coli strain BW25113, a K12 derivative⁷¹ was used for all experiments along with a modified 561 lambda phage strain $(\lambda_{vir})^{72}$ that is locked into the lytic lifestyle. 562 563 564 For all CRISPR interference assays, bacteria were transformed with Cas12a and crRNA 565 expression plasmids by heat shock. Transformants were plated on LB plates containing ampicillin at 100 µg/mL and chloramphenicol at 25 µg/mL to select for plasmids pUC19 and 566 567 pACYCDuet-1, respectively. 568 569 The red operon deletion strain was generated by using 20 μ L of 1:10 diluted λ_{vir} stock to 570 infect E. coli BW25113 cells harboring pUC19 plasmid with a ~800 bp section of the lambda 571 genome inserted in the multiple cloning site with the lambda red operon removed. The culture 572 was grown in 2 mL LB media containing 25 µg/mL ampicillin and 10 mM MgSO₄. After lysis, cell debris was removed by centrifugation and supernatant containing phage was isolated. Phages 573 were then passaged twice through cultures containing E. coli harboring a pACYCDuet-1 574 575 FnCas12a expression plasmid and separate pUC19 plasmid allowing expression of a pre-crRNA

with two spacers targeting different locations in the lambda red operon to select for phage with 576 577 the operon deleted. 20 µL of previously isolated phage lysate was added to each subsequent 578 culture. These 2 mL LB media cultures contained 100 µg/mL ampicillin, 25 µg/mL chloramphenicol, 20 mM arabinose, and 10 mM MgSO₄. Phage lysates were harvested, and 579 deletions were confirmed with PCR amplification of the lambda red operon flanking region and 580 581 Sanger sequencing of the PCR product. 582 583 Phage spot assays Overnight cultures were started using E. coli transformed with Cas12a and crRNA expression 584 plasmids in LB media with ampicillin and chloramphenicol for selection. The next day, 20 µL of 585 these overnight cultures were used to inoculate 2 mL cultures in LB media containing 100 586 587 μg/mL ampicillin, 25 μg/mL chloramphenicol, 20 mM arabinose, and 10 mM MgSO₄. The cultures were grown in a shaking incubator at 200 rpm 37 °C until OD₆₀₀ 0.4 was reached. 300 588 589 μL of cell culture was added to 3 mL 0.7% soft agar containing the same concentrations of 590 ampicillin, chloramphenicol, arabinose and MgSO₄. The cell-soft agar mixture was vortexed for 591 5 seconds and spread onto an LB plate containing ampicillin and chloramphenicol. The plate was dried for 5 minutes. Lambda phage suspended in LB media with 10 mM MgSO₄ was serially 592 593 diluted in seven steps with a 1:10 dilution each step. 2 µL of each phage dilution was then spotted on top of the soft agar layer and the plate was dried for 10 minutes. Plates were incubated 594 595 overnight at 30°C. 596 597 Liquid culture phage assays and growth curves 598 Overnight cultures were started using a single colony of E. coli with Cas12a and crRNA 599 expression plasmids in LB media with ampicillin and chloramphenicol added for selection. The 600 next day, these overnight cultures were used to inoculate cultures 1 to 100 in LB media 601 containing 100 µg/mL ampicillin, 25 µg/mL chloramphenicol, 20 mM arabinose, and 10 mM 602 MgSO₄. The cultures were grown in a shaking incubator at 200 rpm and 37 °C for 1.5 hours until 603 $OD_{600} \sim 0.25$ was reached. 604 Lambda phage was added at MOI 0.02, or as indicated in figure legends. For growth curves, OD 605

readings were immediately taken after addition of the phage and this value represented the "0

607 hour" time point. For growth curves shown in Fig. 1d, Fig. 5a, and S5a, OD was measured at 600 608 nm wavelength every 1 hour in a WPA Biowave CD8000 Cell Density Meter if growing in 609 culture tubes. For growth curves shown in Fig. 6b and S4b, 150 µL cultures were grown in a TECAN infinite M Nano+ 96 well plate reader at 280 rpm and 37 °C and OD measurements at 610 600 nm wavelength were measured every 10 minutes. 611 612 613 Phage plaque assays E. coli bacterial cultures were prepared and induced the same way as in the phage spot assays. 50 614 μL of phage diluted between 1:1 and 1:10⁶ in LB media was added to 300 μL of induced cell 615 culture at OD₆₀₀ 0.4. This mixture was then added to 3 mL 0.7% soft agar containing ampicillin, 616 chloramphenicol, arabinose and MgSO4 as in the phage spot assays and the mixture was vortexed 617 for 5 seconds and spread onto an LB plate containing ampicillin and chloramphenicol. The plate 618 619 was dried for 10 minutes and left to incubate at 37 °C overnight. Plaques were counted the next 620 morning. 621 622 Cas9 and Cas12a expression and purification Cas9 and Cas12a proteins were expressed in E. coli (DE3) cells. LB broth supplemented with 50 623 624 μg/mL kanamycin was inoculated with overnight culture of the cells carrying the expression plasmid in 1:100 ratio. Protein expression was induced by adding 0.5 mM IPTG when the culture 625 626 reached an OD600 of 0.5-0.6. The culture was incubated at 18 °C overnight (about 16 hours) with shaking. 627 628 Cas 9 and Cas 12a were purified by the following protocol, adapted from previous methods with 629 modifications^{53,73}. After harvesting, the cell pellets were resuspended in Lysis Buffer (20 mM 630 631 Tris-HCl, pH 8.0, 500 mM NaCl, 5 mM imidazole and 5% glycerol) supplemented with 1 mM 632 PMSF. The resuspended cells were lysed by sonication and the lysate then was centrifuged to remove insoluble material. The clarified supernatant was transferred to a HisPurTM Ni-NTA resin 633 634 (Thermo Fisher Scientific) column pre-equilibrated with Lysis Buffer without disturbing the 635 pellets. The column was washed with 50 column volumes of Lysis Buffer, then washed again with 50 column volumes of Wash Buffer (20 mM Tris-HCl, pH 8.0, 500 mM NaCl, 15 mM 636 imidazole and 5% glycerol). Elution Buffer (20 mM Tris-HCl, pH 8.0, 500 mM NaCl, 250 mM 637

imidazole and 5% glycerol) was applied to elute bound protein which was collected and cleaved 638 with TEV protease in a 1:100 (w/w) ratio to remove MBP. TEV cleavage reaction was incubated 639 640 overnight at 4oC during dialysis in Dialysis Buffer (10 mM HEPES-KOH, pH 7.5, 200 mM KCl, 1 mM DTT and 5% glycerol). The protein was concentrated and then diluted with Dilution 641 Buffer (20 mM HEPES-KOH, pH 7.5 and 5% glycerol) to a final concentration of 100 mM KCl. 642 643 The protein was loaded on a HiTrap Heparin HP (GE Healthcare) column pre-equilibrated with Buffer A (20 mM HEPES-KOH, pH 7.5, 100 mM KCl and 5% glycerol). The column was 644 washed with 20% of Buffer B (20 mM HEPES-KOH, pH 7.5, 1 M KCl, and 5% glycerol). The 645 protein was eluted with Buffer B by applying a gradient from 20 % to 100% over a total volume 646 of 60 ml. Peak fractions were collected and analyzed by SDS-PAGE. Fractions containing 647 interested protein were combined and concentrated to 1 mL volume. The upper concentrator 648 649 chamber was refilled with SEC buffer (20 mM HEPES-KOH, pH 7.5, 200 mM KCl and 1 mM DTT) and then centrifuged to 1 mL volume (repeated this step 3 times) in order to exchange 650 651 buffer. Finally, the concentrated proteins were aliquoted, flash-frozen in liquid nitrogen and 652 stored at -80 °C. 653 654 crRNA and tracrRNA preparation 655 All crRNAs were in vitro transcribed using short oligonucleotides (IDT) consisting of a T7 promoter region and a template sequence. The oligonucleotides first pre-annealed T7 promoter 656 657 sequence at 90 °C for 2 min and then incubated a room temperate for 10 min. The 500 μL transcription reaction was performed in transcription buffer (40 mM Tris, pH 8.0, 38 mM 658 659 MgCl2, 1 mM Spermidine, pH 8.0, 0.01% Triton X-100, 5 mM ATP, 5 mM CTP, 5 mM GTP, 5 mM UTP, 5 mM DTT) with 0.5 µM pre-annealed DNA and excess of T7 RNA polymerase at 37 660 661 °C for 4 hours. 2X RNA dye was added into the reaction, heated for 5 min at 95oC and then 662 kept on ice. The reaction was run on 10% denaturing acrylamide gel for 3 h with 1X TBE buffer. The crRNA band was visualized under UV-light and was excised from the gel. The gel was 663 crushed and soaked overnight in 1 mL nuclease-free water at 4 °C with rocking. The gel tube 664 665 was centrifuged 5 min at 2000 X g and the supernatant was transferred to Costar Spin-X 666 centrifuge tube filters (Sigma Aldrich). The tube filter was centrifuged at highest speed for 2 min

to collect crRNA solution at the collection chamber. Ethanol precipitation was performed to

667

668

concentrate crRNA.

669 670 tracrRNA were also in vitro synthesized as described above, however, the tracrRNA template 671 was cloned into pUC19 plasmid with an EcoRI restriction site at the end of the template 672 sequence. The tracrRNA plasmid was first linearized with EcoRI and then used as template for in vitro transcription without pre-annealing step. 673 674 In vitro cleavage assays 675 Cleavage assays were prepared in reaction buffer (20 mM HEPES, pH 7.5, 100 mM KCl, 1 mM 676 MgCl₂, 1 mM DTT and 5% glycerol) with a final concentration of 50 nM FnCas12a or SpCas9. 677 FnCas12a RNP complex was formed by incubating FnCas12a and crRNA at a 1:1.5 ratio at 37 678 °C for 10 min. Cas9 RNP complex was formed by incubating Cas9:crRNA:tracRNA at a 679 1:1.5:1.5 ratio at 37 °C for 10 min. To initiate cleavage, target plasmid was added to a final 680 concentration of 15 ng/µl and a final reaction volume of 100 µl. The reaction was incubated at 37 °C. Aliquots (10 µl) were quenched at 7, 15, 30, 60, 300, 900 and 1800 s by adding 10 µl phenol-681 682 chloroform-isoamyl alcohol (25:24:1 v/v, Invitrogen). After phenol-chloroform extraction, DNA 683 products were separated by electrophoresis on a 1% agarose gel, and visualized with SYBR Safe (Invitrogen) staining. The densitometry of individual DNA bands was measured in ImageJ 684 685 (https://imagej.nih.gov/ij/). The fraction cleaved was determined by dividing the total cleaved DNA (nicked and linearized DNA) by total DNA (nicked, linearized and supercoiled DNA). 686 Fraction cleaved was plotted versus time and fit to a first-order rate equation to determine an 687 688 observed rate constant for cleavage ($k_{\rm obs}$). Rates were measured in triplicate. 689 690 High-throughput sequencing sample preparation 691 Phage samples were isolated from spots in spot assays at the highest phage dilution in which a cleared spot was observed to ensure a diverse population of mutant phages would be sampled. A 692 693 1 mL pipette tip was poked through a phage spot and the agar in the tip is suspended in 30 μL 694 deionized H₂O in a 1.5 mL microcentrifuge tube and incubated in a 48°C water bath for 20 695 minutes to melt the agar and dissolve the phage particles. The tubes were vortexed briefly and 696 incubated in the water bath for another 10 minutes. The water/melted agar mixture that contains 697 the phage was removed.

For phage samples from liquid culture, 50 µL of each culture was transferred to a 1.5 mL tube and bacteria were pelleted from the liquid culture by centrifuging at 15,000 rpm for 5 minutes.

The supernatant containing phage particles was then removed.

702

703704

705

706

707

708

709

710

699

700

701

5 μL of phage solution was used as the template for a 25 cycle PCR reaction with primers containing Nextera adapters. These PCR products were cleaned up using the Promega Wizard PCR purification kit and used as a template for an 8 cycle PCR reaction to add barcodes for sample identification. Q5 DNA polymerase (New England Biolabs) was used for all adapter and barcode PCR reactions. Samples were pooled and gel purified using the Promega Wizard PCR purification kit. Gel purified samples were then submitted for MiSeq high-throughput sequencing. Conditions for MiSeq runs were Nextera DNA MiSEQ 150-Cycle which included two 75 base pair paired end reads. Adapter PCR primers were designed so both of the paired R1

711712

713

714

Samples were prepared for PacBio sequencing by 35 cycle PCR amplification of phage samples isolated from liquid culture. PCR products were purified using the Promega Wizard PCR purification kit and submitted for Pacbio sequencing.

715716

717

High-throughput sequencing data processing

- A script written in Python 3.8 was used to process fastq data files received from a MiSeq run.
- 719 The script extracts target region sequences and determines if the target region contains a

and R2 reads overlapped in the entire protospacer region including the PAM.

- mutation relative to the wild-type target sequence. Base substitutions and deletions were
- 721 classified along with the location of the substitution or deletion relative to the PAM sequence of
- 722 the target. Mutations were also classified based on the type of mutation (A to C for example). A
- Microsoft Excel sheet was then created with the data using the "Xlsxwriter" Python package⁷⁴.
- 724 Z-score calculations and heat maps for each sample were created using Microsoft Excel. Z-
- scores for each position in the phage target regions were calculated using the average proportion
- of reads with mutations at each position in experimental samples x and control samples μ and the
- standard deviation of the proportion of mutations at all positions in all
- 728 Samples σ .

$$Z = \frac{\underline{x} - \underline{\mu}}{\sigma} \qquad (Eq. 1)$$

A separate script written in Python 3.8 was used to process data files received from PacBio highthroughput sequencing and find deletions in the lambda phage genome. Sequences were extracted from fastq files and matched piecewise to the WT sequence of the genome region that was PCR amplified. Deletions are output as coordinates in the PCR amplified region and these coordinates were translated to the lambda phage genome to create the bar graph in Fig. 7b.

Nucleotide diversity was calculated using the proportion of all pairs of sequences x_i and x_j in each sample and the number of nucleotide differences between each pair of sequences π_{ij} divided by the length of the PAM and protospacer region (24).

 $Diversity = \frac{1}{24} \sum_{i=2}^{n} \sum_{j=1}^{i-1} 2x_i x_j \pi_{ij} \quad (Eq. 2)$

Find the scripts at https://github.com/alexsq2/lambda-phage-CRISPR-mutants

Generation and purification of mutant phage

The gene L A2T mutant phage reported in Fig. 3 was generated on solid media by isolation of single plaques. In this case, 300 μL of *E. coli* BW25113 transformed with the FnCas12a and MM15 crRNA expression plasmids at OD600 ~0.4 was added to 3 mL 0.7% agar containing 100 μg/mL ampicillin, 25 μg/mL chloramphenicol, 20 mM arabinose, and 10 mM MgSO4, and 20 μL of undiluted WT phage lysate. Soft agar was vortexed for 5 s and poured onto LB agar plates containing the same concentrations of ampicillin and chloramphenicol. Plates were incubated at 37 °C overnight. Phage was isolated from a single plaque by poking into the plaque with a 1 mL pipette tip and the agar was suspended in 20 μL deionized H2O in a 1.5 mL microcentrifuge tube and incubated in a 48 °C water bath for ~20 minutes. Soft agar containing phage was transferred to a fresh 1.5 mL tube.

For mutants reported in Fig. 7, overnight cultures were started using a single colony of *E. coli* with Cas12a and indicated crRNA expression plasmids in LB media with ampicillin and chloramphenicol added for selection. The next day, these overnight cultures were used to inoculate cultures 1 to 100 in LB media containing 100 μg/mL ampicillin, 25 μg/mL chloramphenicol, 20 mM arabinose, and 10 mM MgSO4. The cultures were grown in a shaking incubator at 200 rpm 37 °C for 1.5 hours until OD₆₀₀ ~0.4 was reached. Lambda phage was added at MOI 0.02. Cultures continued to grow in the shaking incubator for 5 hours. Cultures

were transferred to 1.5ml tubes and centrifuged at 5000 rpm for 5 minutes. Supernatant containing phage was transferred to a fresh 1.5 mL tube.

In both cases, phage was then diluted and used for phage plaque assays on lawns of bacteria expressing the same crRNA as in the previous infection to select against remaining WT phage. Single plaques were isolated and used to infect bacterial cultures again expressing the same crRNA under the same conditions as described above. Cultures were grown in a shaking incubator at 200 rpm 37 °C for 5 hours. 5 µL of phage solution was then used as a template for a 35 cycle PCR reaction with Phusion polymerase to amplify the target region. Sanger sequencing was used to confirm the presence and purity of mutations in the target region.

Mutant Phage Competition Assay

Single mutant phages were purified as in "Generation and purification of mutant phage". Two different mutant phage lysates were mixed in 1:2 and 2:1 ratios by titer and these mixes were serially diluted 1:10 in seven dilution steps in LB media containing 10 mM MgSO4. 3 µL of each dilution was added to 150 µL E. coli BW25113 cultures at OD600 0.4 with cells harboring a pACYCDuet-1 FnCas12a expression plasmid and separate pUC19 plasmid allowing expression of a pre-crRNA targeting the region of the lambda phage genome containing the mutation. These 150 µL LB media cultures contained 100 µg/mL ampicillin, 25 µg/mL chloramphenicol, 20 mM arabinose, and 10 mM MgSO4. Complete lysis was observed for all cultures at 8 h after infection and phage lysates were isolated by centrifugation and removal of the supernatant. Sequencing samples were prepared as in "High-throughput sequencing sample preparation" to determine the proportion of each mutant phage in each sample. Ratio of seed:PAM-distal mutants in the population were determined by dividing the number of reads for the seed mutant by the number of reads for the PAM-distal mutant for each sample.

Sanger sequencing of phage plaques or phage lysate

Phage was isolated from a single plaque by poking into the plaque with a 1 mL pipette tip and the agar was suspended in 20 µL deionized H₂O in a 1.5 mL microcentrifuge tube and incubated in a 48°C water bath for ~20 minutes. Melted agar and H₂O mixture containing phages was transferred to a 1.5 mL microcentrifuge tube.

- 792
- 793 Phage was also isolated from liquid cultures by transferring 1ml of liquid culture to a 1.5 mL
- microcentrifuge tube and centrifuging at 15,000 rpm for 5 minutes. Supernatant containing
- 795 phages was transferred to a clean 1.5 mL microcentrifuge tube.

796

- 797 5 μL of phage solution was used as a template for a PCR reaction that amplifies the target region
- in the middle of a ~800 base pair PCR product. One of the primers used for the PCR reaction
- was used for sequencing of the PCR product.

800 Acknowledgements

- We thank Michael Baker and Kevin Cavallin of the Iowa State DNA Facility for advice on
- 802 MiSeq sample preparation and data processing. MiSeq sequencing was performed at the Iowa
- State DNA Facility and PacBio sequencing was performed by the DNA Sequencing Center of
- 804 Brigham Young University. Financial support for this research was provided by National
- Science Foundation award 1652661 (to D.G.S.).

806 References

- 1. Grissa, I., Vergnaud, G. & Pourcel, C. The CRISPRdb database and tools to display
- CRISPRs and to generate dictionaries of spacers and repeats. *BMC Bioinformatics* **8**, 172
- 809 (2007).
- 2. Godde, J. S. & Bickerton, A. The repetitive DNA elements called CRISPRs and their
- associated genes: evidence of horizontal transfer among prokaryotes. J Mol Evol 62, 718–
- 812 729 (2006).
- 3. Makarova, K. S. *et al.* Evolutionary classification of CRISPR–Cas systems: a burst of class 2
- and derived variants. *Nature Reviews Microbiology* **18**, 67–83 (2020).
- 4. Sorek, R., Lawrence, C. M. & Wiedenheft, B. CRISPR-Mediated Adaptive Immune Systems
- in Bacteria and Archaea. *Annual Review of Biochemistry* **82**, 237–266 (2013).

- 5. Mohanraju, P. et al. Diverse evolutionary roots and mechanistic variations of the CRISPR-
- 818 Cas systems. *Science* **353**, (2016).
- 819 6. Johnke, J. et al. Multiple micro-predators controlling bacterial communities in the
- environment. *Curr Opin Biotechnol* **27**, 185–190 (2014).
- 7. Fuhrman, J. A. Marine viruses and their biogeochemical and ecological effects. *Nature* **399**,
- 822 541–548 (1999).
- 823 8. Wommack, K. E., Ravel, J., Hill, R. T. & Colwell, R. R. Hybridization Analysis of
- Chesapeake Bay Virioplankton. *Appl Environ Microbiol* **65**, 241–250 (1999).
- 9. Avrani, S., Wurtzel, O., Sharon, I., Sorek, R. & Lindell, D. Genomic island variability
- facilitates Prochlorococcus–virus coexistence. *Nature* **474**, 604–608 (2011).
- 10. Deveau, H. et al. Phage Response to CRISPR-Encoded Resistance in Streptococcus
- thermophilus. *Journal of Bacteriology* **190**, 1390–1400 (2008).
- 11. Datsenko, K. A. et al. Molecular memory of prior infections activates the CRISPR/Cas
- adaptive bacterial immunity system. *Nat Commun* **3**, 945 (2012).
- 12. Sun, C. L. et al. Phage mutations in response to CRISPR diversification in a bacterial
- population. *Environmental Microbiology* **15**, 463–470 (2013).
- 13. Rossetti, G. et al. The structural impact of DNA mismatches. Nucleic Acids Res 43, 4309–
- 834 4321 (2015).
- 835 14. Sugimoto, N., Nakano, M. & Nakano, S. Thermodynamics—Structure Relationship of Single
- Mismatches in RNA/DNA Duplexes. *Biochemistry* **39**, 11270–11281 (2000).
- 15. Borer, P. N., Dengler, B., Tinoco, I. & Uhlenbeck, O. C. Stability of ribonucleic acid double-
- stranded helices. *Journal of Molecular Biology* **86**, 843–853 (1974).
- 16. Feng, H., Guo, J., Wang, T., Zhang, C. & Xing, X. Guide-target mismatch effects on dCas9–

- sgRNA binding activity in living bacterial cells. *Nucleic Acids Research* **49**, 1263–1277
- 841 (2021).
- 17. Meeske, A. J., Nakandakari-Higa, S. & Marraffini, L. A. Cas13-induced cellular dormancy
- prevents the rise of CRISPR-resistant bacteriophage. *Nature* 1 (2019) doi:10.1038/s41586-
- 844 019-1257-5.
- 18. Zheng, Y. et al. Endogenous Type I CRISPR-Cas: From Foreign DNA Defense to
- Prokaryotic Engineering. Frontiers in Bioengineering and Biotechnology 8, (2020).
- 19. Chylinski, K., Makarova, K. S., Charpentier, E. & Koonin, E. V. Classification and evolution
- of type II CRISPR-Cas systems. *Nucleic Acids Res* **42**, 6091–6105 (2014).
- 20. Li, Y. et al. Cmrl enables efficient RNA and DNA interference of a III-B CRISPR-Cas
- system by binding to target RNA and crRNA. *Nucleic Acids Res* **45**, 11305–11314 (2017).
- 851 21. Wang, R. & Li, H. The mysterious RAMP proteins and their roles in small RNA-based
- immunity. *Protein Sci* **21**, 463–470 (2012).
- 22. Kolesnik, M. V., Fedorova, I., Karneyeva, K. A., Artamonova, D. N. & Severinov, K. V.
- Type III CRISPR-Cas Systems: Deciphering the Most Complex Prokaryotic Immune
- 855 System. *Biochemistry Moscow* **86**, 1301–1314 (2021).
- 23. Vercoe, R. B. *et al.* Cytotoxic Chromosomal Targeting by CRISPR/Cas Systems Can
- Reshape Bacterial Genomes and Expel or Remodel Pathogenicity Islands. *PLOS Genetics* **9**,
- 858 e1003454 (2013).
- 859 24. Mojica, F. J. M., Díez-Villaseñor, C., García-Martínez, J. & Almendros, C. Short motif
- sequences determine the targets of the prokaryotic CRISPR defence system. *Microbiology*,
- 861 **155**, 733–740 (2009).
- 25. Sternberg, S. H., Redding, S., Jinek, M., Greene, E. C. & Doudna, J. A. DNA interrogation

- by the CRISPR RNA-guided endonuclease Cas9. *Nature* **507**, 62–67 (2014).
- 26. Zetsche, B. et al. Cpf1 Is a Single RNA-Guided Endonuclease of a Class 2 CRISPR-Cas
- 865 System. *Cell* **163**, 759–771 (2015).
- 27. Horvath, P. et al. Diversity, Activity, and Evolution of CRISPR Loci in Streptococcus
- thermophilus. *Journal of Bacteriology* **190**, 1401–1412 (2008).
- 28. Pattanayak, V. et al. High-throughput profiling of off-target DNA cleavage reveals RNA-
- programmed Cas9 nuclease specificity. *Nature Biotechnology* **31**, 839–843 (2013).
- 29. Cong, L. et al. Multiplex Genome Engineering Using CRISPR/Cas Systems. Science 339,
- 871 819–823 (2013).
- 30. Künne, T., Swarts, D. C. & Brouns, S. J. J. Planting the seed: target recognition of short
- guide RNAs. *Trends in Microbiology* **22**, 74–83 (2014).
- 31. Semenova, E. et al. Interference by clustered regularly interspaced short palindromic repeat
- (CRISPR) RNA is governed by a seed sequence. *PNAS* **108**, 10098–10103 (2011).
- 876 32. Jiang, W., Bikard, D., Cox, D., Zhang, F. & Marraffini, L. A. RNA-guided editing of
- bacterial genomes using CRISPR-Cas systems. *Nat Biotechnol* **31**, 233–239 (2013).
- 878 33. Maier, L.-K. et al. Essential requirements for the detection and degradation of invaders by
- the Haloferax volcanii CRISPR/Cas system I-B. RNA Biology 10, 865–874 (2013).
- 880 34. Wiedenheft, B. et al. RNA-guided complex from a bacterial immune system enhances target
- recognition through seed sequence interactions. PNAS 108, 10092–10097 (2011).
- 882 35. Tao, P., Wu, X. & Rao, V. Unexpected evolutionary benefit to phages imparted by bacterial
- 883 CRISPR-Cas9. *Science Advances* **4**, eaar4134 (2018).
- 36. Chabas, H. et al. Variability in the durability of CRISPR-Cas immunity. *Philosophical*
- 885 Transactions of the Royal Society B: Biological Sciences 374, 20180097 (2019).

- 886 37. Pereira-Gómez, M. & Sanjuán, R. Effect of mismatch repair on the mutation rate of
- bacteriophage \$\phi X174\$. Virus Evolution 1, vev010 (2015).
- 38. Wu, X., Zhu, J., Tao, P. & Rao, V. B. Bacteriophage T4 Escapes CRISPR Attack by
- Minihomology Recombination and Repair. *mBio* **12**, e01361-21.
- 39. Hossain, A. A., McGinn, J., Meeske, A. J., Modell, J. W. & Marraffini, L. A. Viral
- recombination systems limit CRISPR-Cas targeting through the generation of escape
- mutations. *Cell Host & Microbe* **29**, 1482-1495.e12 (2021).
- 40. Mojica, F. J. M., Díez-Villaseñor, C., García-Martínez, J. & Soria, E. Intervening Sequences
- of Regularly Spaced Prokaryotic Repeats Derive from Foreign Genetic Elements. *J Mol Evol*
- **60**, 174–182 (2005).
- 41. Bolotin, A., Quinquis, B., Sorokin, A. & Ehrlich, S. D. Clustered regularly interspaced short
- palindrome repeats (CRISPRs) have spacers of extrachromosomal origin. *Microbiology* **151**,
- 898 2551–2561 (2005).
- 42. Heidelberg, J. F., Nelson, W. C., Schoenfeld, T. & Bhaya, D. Germ Warfare in a Microbial
- 900 Mat Community: CRISPRs Provide Insights into the Co-Evolution of Host and Viral
- 901 Genomes. *PLOS ONE* **4**, e4169 (2009).
- 902 43. Semenova, E., Nagornykh, M., Pyatnitskiy, M., Artamonova, I. I. & Severinov, K. Analysis
- of CRISPR system function in plant pathogen Xanthomonas oryzae. FEMS Microbiol Lett
- 904 **296**, 110–116 (2009).
- 905 44. Pourcel, C., Salvignol, G. & Vergnaud, G. CRISPR elements in Yersinia pestis acquire new
- repeats by preferential uptake of bacteriophage DNA, and provide additional tools for
- 907 evolutionary studies. *Microbiology* **151**, 653–663 (2005).
- 908 45. Andersson, A. F. & Banfield, J. F. Virus Population Dynamics and Acquired Virus

- Resistance in Natural Microbial Communities. *Science* **320**, 1047–1050 (2008).
- 910 46. Sun, C. L., Thomas, B. C., Barrangou, R. & Banfield, J. F. Metagenomic reconstructions of
- bacterial CRISPR loci constrain population histories. *ISME J* **10**, 858–870 (2016).
- 47. Nussenzweig, P. M., McGinn, J. & Marraffini, L. A. Cas9 Cleavage of Viral Genomes
- Primes the Acquisition of New Immunological Memories. *Cell Host & Microbe* **26**, 515-
- 914 526.e6 (2019).
- 48. Fineran, P. C. et al. Degenerate target sites mediate rapid primed CRISPR adaptation. Proc
- 916 *Natl Acad Sci U S A* **111**, E1629-1638 (2014).
- 917 49. Xue, C. *et al.* CRISPR interference and priming varies with individual spacer sequences.
- 918 *Nucleic Acids Res* **43**, 10831–10847 (2015).
- 50. Xue, C., Whitis, N. R. & Sashital, D. G. Conformational Control of Cascade Interference and
- Priming Activities in CRISPR Immunity. *Mol Cell* **64**, 826–834 (2016).
- 921 51. Cho, S. W. et al. Analysis of off-target effects of CRISPR/Cas-derived RNA-guided
- 922 endonucleases and nickases. *Genome Res.* **24**, 132–141 (2014).
- 52. Hsu, P. D. et al. DNA targeting specificity of RNA-guided Cas9 nucleases. *Nature*
- 924 *Biotechnology* **31**, 827–832 (2013).
- 925 53. Murugan, K., Seetharam, A. S., Severin, A. J. & Sashital, D. G. CRISPR-Cas12a has
- widespread off-target and dsDNA-nicking effects. *J. Biol. Chem.* jbc.RA120.012933 (2020)
- 927 doi:10.1074/jbc.RA120.012933.
- 54. Strohkendl, I., Saifuddin, F. A., Rybarski, J. R., Finkelstein, I. J. & Russell, R. Kinetic Basis
- for DNA Target Specificity of CRISPR-Cas12a. *Molecular Cell* **71**, 816-824.e3 (2018).
- 930 55. Jinek, M. et al. A Programmable Dual-RNA–Guided DNA Endonuclease in Adaptive
- 931 Bacterial Immunity. *Science* **337**, 816–821 (2012).

- 932 56. Jones, S. K. *et al.* Massively parallel kinetic profiling of natural and engineered CRISPR
- 933 nucleases. *Nature Biotechnology* 1–10 (2020) doi:10.1038/s41587-020-0646-5.
- 57. Kleinstiver, B. P. et al. Genome-wide specificities of CRISPR-Cas Cpf1 nucleases in human
- 935 cells. *Nature Biotechnology* **34**, 869–874 (2016).
- 58. Endo, A., Masafumi, M., Kaya, H. & Toki, S. Efficient targeted mutagenesis of rice and
- tobacco genomes using Cpf1 from Francisella novicida. Sci Rep 6, 38169 (2016).
- 938 59. Alok, A. et al. The Rise of the CRISPR/Cpf1 System for Efficient Genome Editing in Plants.
- 939 Frontiers in Plant Science 11, (2020).
- 940 60. Kim, D. et al. Genome-wide analysis reveals specificities of Cpf1 endonucleases in human
- 941 cells. *Nature Biotechnology* **34**, 863–868 (2016).
- 942 61. Zhong, Z. et al. Plant Genome Editing Using FnCpf1 and LbCpf1 Nucleases at Redefined
- and Altered PAM Sites. *Mol Plant* **11**, 999–1002 (2018).
- 62. Chen, J. S. et al. CRISPR-Cas12a target binding unleashes indiscriminate single-stranded
- DNase activity. *Science* **360**, 436–439 (2018).
- 946 63. Phan, P. T., Schelling, M., Xue, C. & Sashital, D. G. Fluorescence-based methods for
- measuring target interference by CRISPR-Cas systems. *Methods Enzymol* **616**, 61–85
- 948 (2019).
- 949 64. Liu, Y. et al. Covalent Modifications of the Bacteriophage Genome Confer a Degree of
- Resistance to Bacterial CRISPR Systems. *J Virol* **94**, e01630-20 (2020).
- 951 65. Gasiunas, G., Barrangou, R., Horvath, P. & Siksnys, V. Cas9-crrna ribonucleoprotein
- complex mediates specific DNA cleavage for adaptive immunity in bacteria. *Proceedings of*
- 953 the National Academy of Sciences 109, (2012).
- 954 66. Barrangou, R. et al. CRISPR Provides Acquired Resistance Against Viruses in Prokaryotes.

- 955 Science **315**, 1709–1712 (2007).
- 956 67. van Houte, S. et al. The diversity-generating benefits of a prokaryotic adaptive immune
- 957 system. *Nature* **532**, 385–388 (2016).
- 68. Held, N. L. & Whitaker, R. J. Viral biogeography revealed by signatures in Sulfolobus
- 959 islandicus genomes. Environ Microbiol 11, 457–466 (2009).
- 960 69. Zoephel, J. RNA-Seq analyses reveal CRISPR RNA processing and regulation patterns.
- 961 *Biochem Soc Trans* **41**, (2013).
- 962 70. Pyenson, N. C. & Marraffini, L. A. Co-evolution within structured bacterial communities
- results in multiple expansion of CRISPR loci and enhanced immunity. *eLife* **9**, e53078
- 964 (2020).
- 71. Baba, T. et al. Construction of Escherichia coli K-12 in-frame, single-gene knockout
- mutants: the Keio collection. Mol Syst Biol 2, 2006.0008 (2006).
- 72. Jacob, F. & Wollman, E. L. [Processes of conjugation and recombination in Escherichia coli.
- I. Induction by conjugation or zygotic induction]. *Ann Inst Pasteur (Paris)* **91**, 486–510
- 969 (1956).

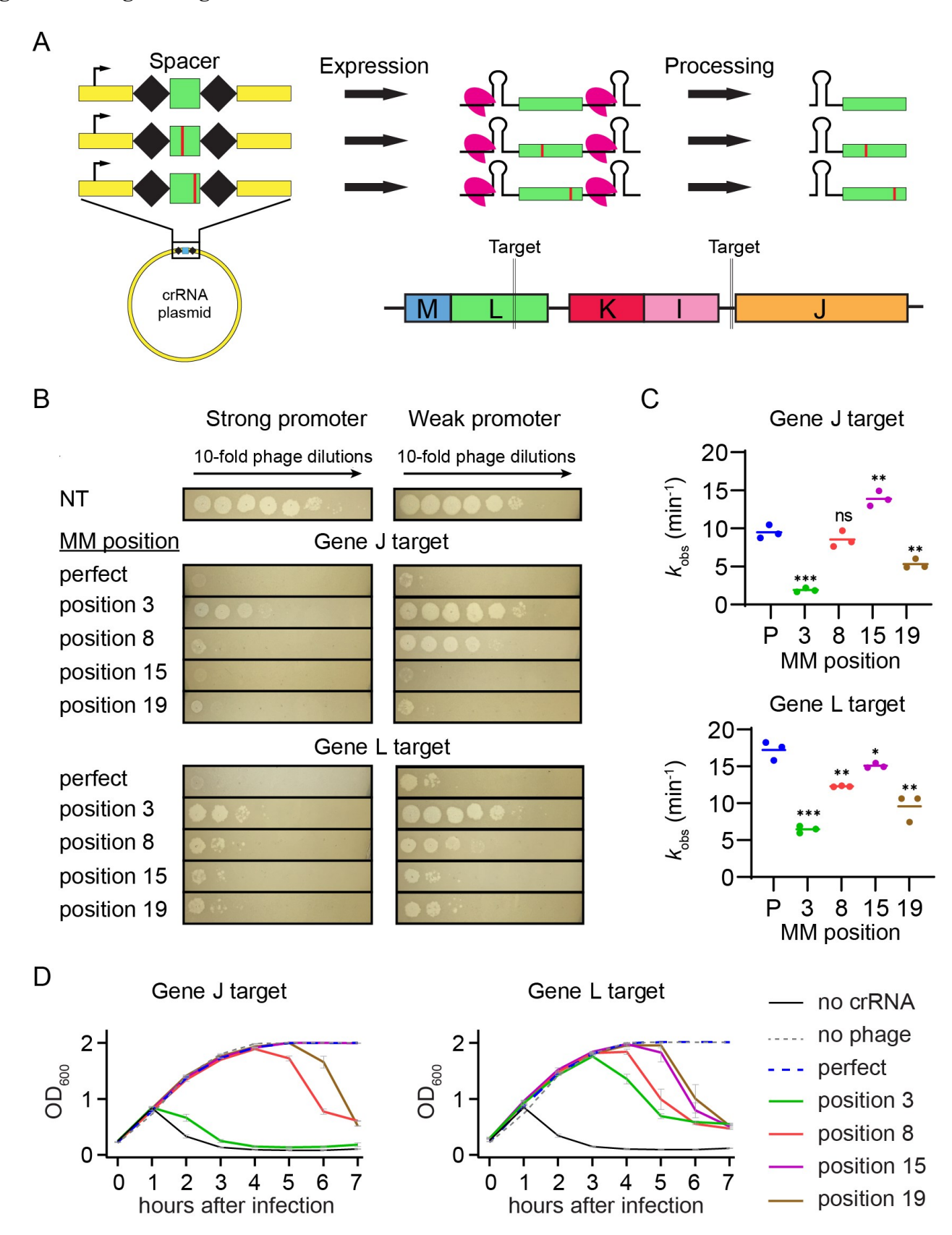
975

- 970 73. Murugan, K., Suresh, S. K., Seetharam, A. S., Severin, A. J., & Sashital, D. G. Systematic in
- 971 *vitro* specificity profiling reveals nicking defects in natural and engineered CRISPR–cas9
- 972 variants. *Nucleic Acids Research*, 49(7), 4037–4053, (2021).
- 973 74. Creating Excel files with Python and XlsxWriter XlsxWriter Documentation.
- https://xlsxwriter.readthedocs.io/index.html.

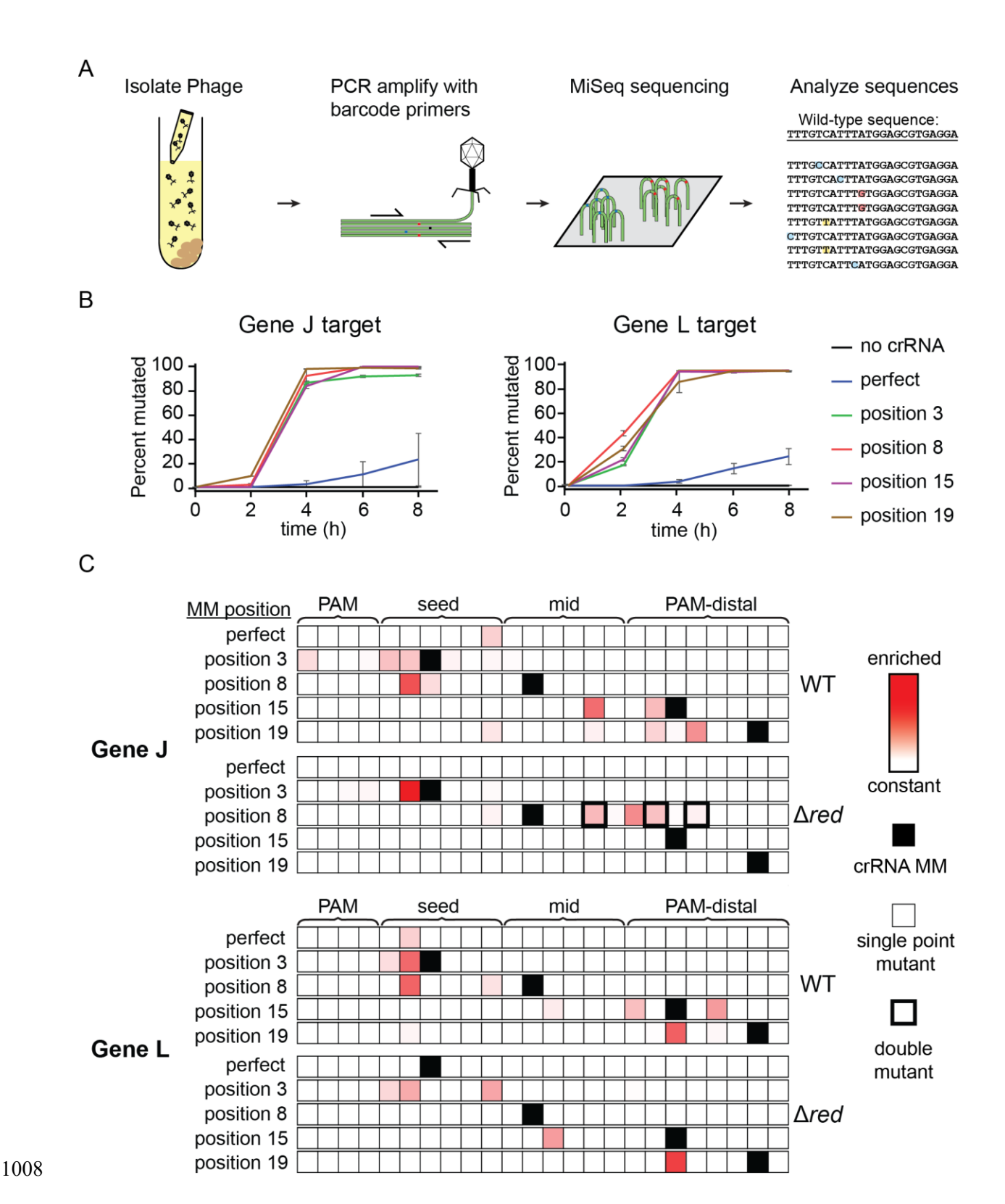
976 Supporting Information Legends

977 Supporting Information: List of plasmids, primers and oligonucleotides used in this study.

979 Figures and Figure Legends



981 Figure 1 - Effects of mismatched crRNAs on Cas12a-mediated phage defense 982 (A) Schematic of crRNA expression and processing by FnCas12a and crRNA phage target 983 locations. crRNA mismatches were introduced by mutating individual nucleotides in the spacer 984 sequence. After expression of the pre-crRNA, Cas12a processes it into a guiding crRNA that partially matches the lambda phage genome targets upstream of gene J and in the coding region 985 986 of gene L. See S1a for target and crRNA spacer sequences. 987 (B) Measurement of phage protection provided by crRNAs with and without target mismatches. 988 Spot assays were performed with bacteria expressing FnCas12a and a crRNA construct that 989 either perfectly matches the lambda phage genome (perfect) or has a crRNA mismatch (MM) at 990 a position in the spacer (position x, sequences shown in S1a Fig.). A non-targeting crRNA 991 construct (NT) was used as a negative control. Lambda phage was spotted on cells with 10-fold 992 decreasing concentration at each spot going from left to right. Expression of FnCas12a and pre-993 crRNAs were controlled by a stronger inducible P_{BAD} promoter or a weaker constitutive 994 promoter. 995 (C) Observed rate constants for in vitro cleavage by Cas12a armed with crRNAs containing 996 target mismatches. Plasmids bearing target sequences for gene J or L were used to measure 997 Cas 12a cleavage. Mismatch positions or perfect crRNAs (P) are indicated on the horizontal axis. Data from three replicates are plotted. * $P \le 0.05$, ** $P \le 0.01$, *** $P \le 0.001$, ns = no significant 998 difference compared to the perfect crRNA based on unpaired two-tailed t-test. See S1b-c for gels 999 1000 and quantification. See S1 Fig. for crRNA and target sequences, representative gels, and fit data. 1001 (D) Growth curves for *E. coli* expressing mismatched crRNAs following phage infection. 1002 Bacteria containing the P_{BAD} FnCas12a expression plasmid and various crRNA expression 1003 plasmids were inoculated in liquid culture and induced immediately. Lambda phage was added 1004 1.5 hours after inoculation and OD₆₀₀ measurements were taken every hour. Bacteria expressed no cRNA, a crRNA with no mismatches to the target (perfect) or a crRNA with a mismatch at 1005 1006 the indicated position (position x). A no phage condition was performed as a negative control. The average of two replicates is plotted, with error bars representing standard deviation. 1007



1009	Figure 2 - crRNA mismatches cause emergence of diverse lambda phage mutations
1010	(A) Schematic of workflow for determining the genetic diversity of phage exposed to
1011	interference by Cas12a. Phage samples were collected from liquid cultures at various time points
1012	and the target region was PCR amplified. Mutations were observed using MiSeq high-throughput
1013	sequencing of these amplicons.
1014	(B) Line graph tracking the fraction of phage with mutated target sequences over time. Samples
1015	were taken from liquid cultures at time points after phage infection. The "0 h" samples were
1016	taken directly after addition of phage to the culture tubes. The average of two replicates are
1017	plotted with error bars representing standard deviation.
1018	(C) Heat maps showing the location of enriched phage mutations in target regions at the 8 h time
1019	point for gene J or L targets. Z-scores for abundance of single-nucleotide variants, including
1020	nucleotide identity changes or deletions, were determined for each sample relative to the non-
1021	targeted control phage population. Experiments were performed using λ_{vir} phage (WT) and λ_{vir}
1022	phage with the red operon deleted (Δred). Enriched sequences indicate high Z-scores. Z-scores
1023	range from 0 (white) to 10.3 (darkest red). Single nucleotide deletions are shown at adjacent
1024	position to the 3' side. Positions with crRNA mismatches are labeled with solid black boxes in
1025	the heat map. A thin outline indicates that the majority of sequences contain single point
1026	mutations at these positions while a thick outline indicates that the majority of sequences contain
1027	multiple point mutations at these positions.

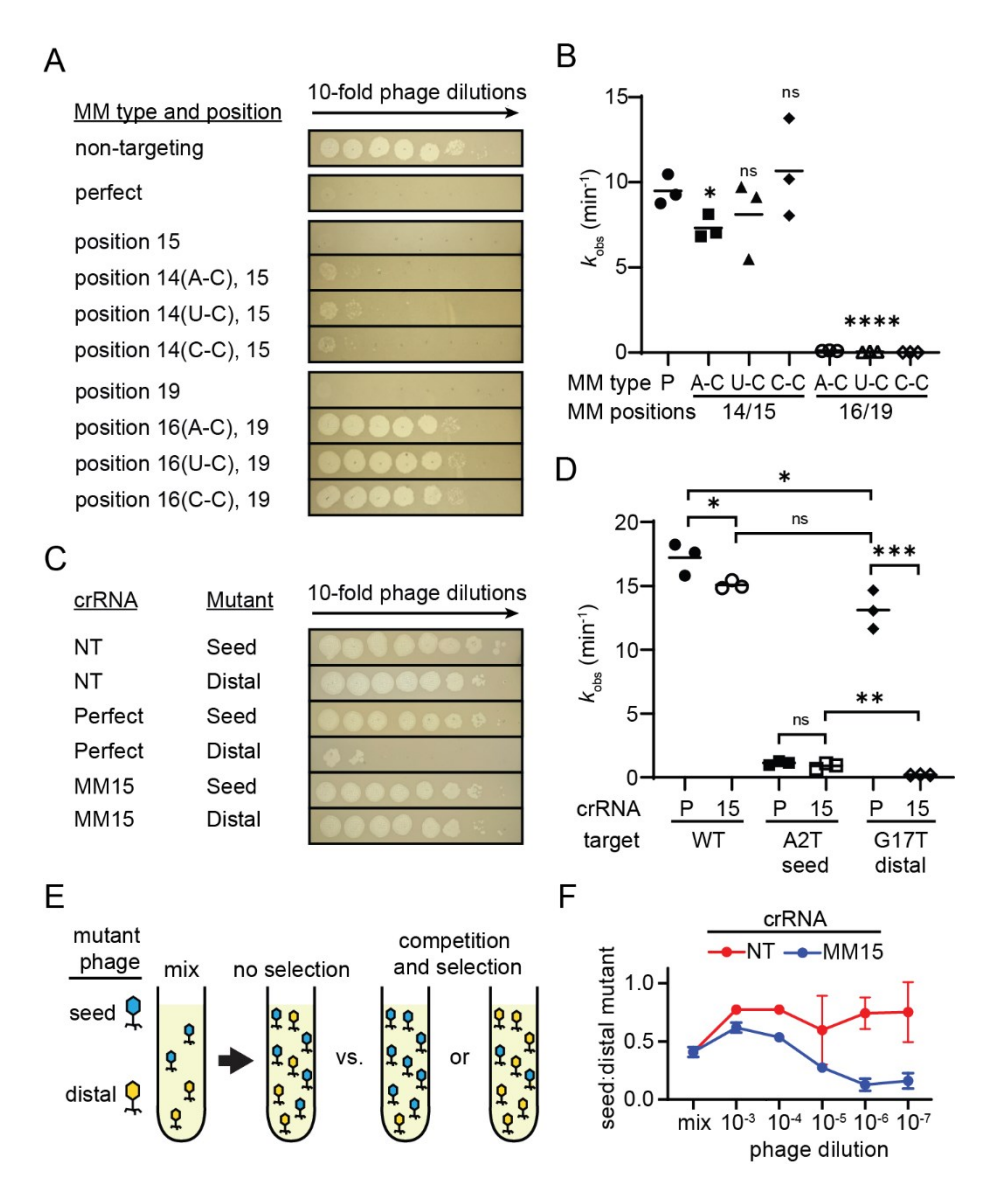


Figure 3 - Two PAM distal mismatches are more deleterious than seed mismatches

(A) Spot assays performed using E. coli expressing FnCas12a and a crRNA that perfectly matches the lambda phage gene J target (perfect) or has mismatches at the indicated positions. Three types of second mismatches were added and the type of the mismatch is indicated in parenthesis next to the position number. See S7a Fig. for crRNA spacer sequences.

(B) Observed rate constants for in vitro cleavage by Cas12a armed with crRNAs containing two target mismatches. Cleavage was measured for plasmid DNA containing a gene J target. The types of mismatches for the second mismatch are indicated. $*P \le 0.05$, $****P \le 0.0001$, ns P > 0.05 compared to the perfectly matching crRNA based on unpaired two-tailed t-test. See S7b-c Fig. for gels and fit data.

- 1039 (C) Phage spot assays for target mutant phages isolated upon challenge with Cas12a
- programmed with a position 15 mismatched crRNA targeting gene L. Spot assays were
- performed with *E. coli* expressing a non-targeting crRNA (NT), a crRNA that perfectly matched
- wild-type phage (Perfect), or the crRNA with a mismatch at position 15 (MM15). Phage
- mutations were in the seed (A2T) or PAM-distal (G17T) region.
- 1044 (D) Observed rate constants for in vitro Cas 12a cleavage of plasmids bearing wild-type (WT),
- seed mutant (A2T), or PAM-distal mutant (G17T) gene L target sequences. Cas12a cleavage was
- measured for both the perfectly matched crRNA (P) or the MM15 crRNA (15). Significance was
- 1047 tested pairwise for all crRNA/target combination by unpaired two-tailed t-test. * $P \le 0.05$, ** $P \le 0.05$
- 1048 0.01, *** $P \le 0.001$, ns P > 0.05. Pairwise comparisons for which P value are not indicated had a
- 1049 P < 0.0001. See S8 Fig. for crRNA and target sequences, gels, and fit data.
- 1050 (E) Schematic of competition assay. Two mutant phages, A2T and G17T, were mixed at
- approximately equal titers. E. coli expressing Cas12a and the position 15 mismatched crRNA
- were infected with a dilution series of the mutant phage mix. Lysates were harvested and the
- proportion of each mutant phage was determined by high-throughput sequencing.
- 1054 (F) Ratio of seed mutant (A2T) to PAM-distal mutant (G17T) following lysis of cultures infected
- with a dilution series of the mixed phage. E. coli expressed Cas12a and either a non-targeting
- 1056 (NT, red) or position 15 mismatched (MM15, blue) crRNA. "Mix" indicates the initial mixture
- of phage. The average of three replicates is shown, with error bars indicating standard deviation.

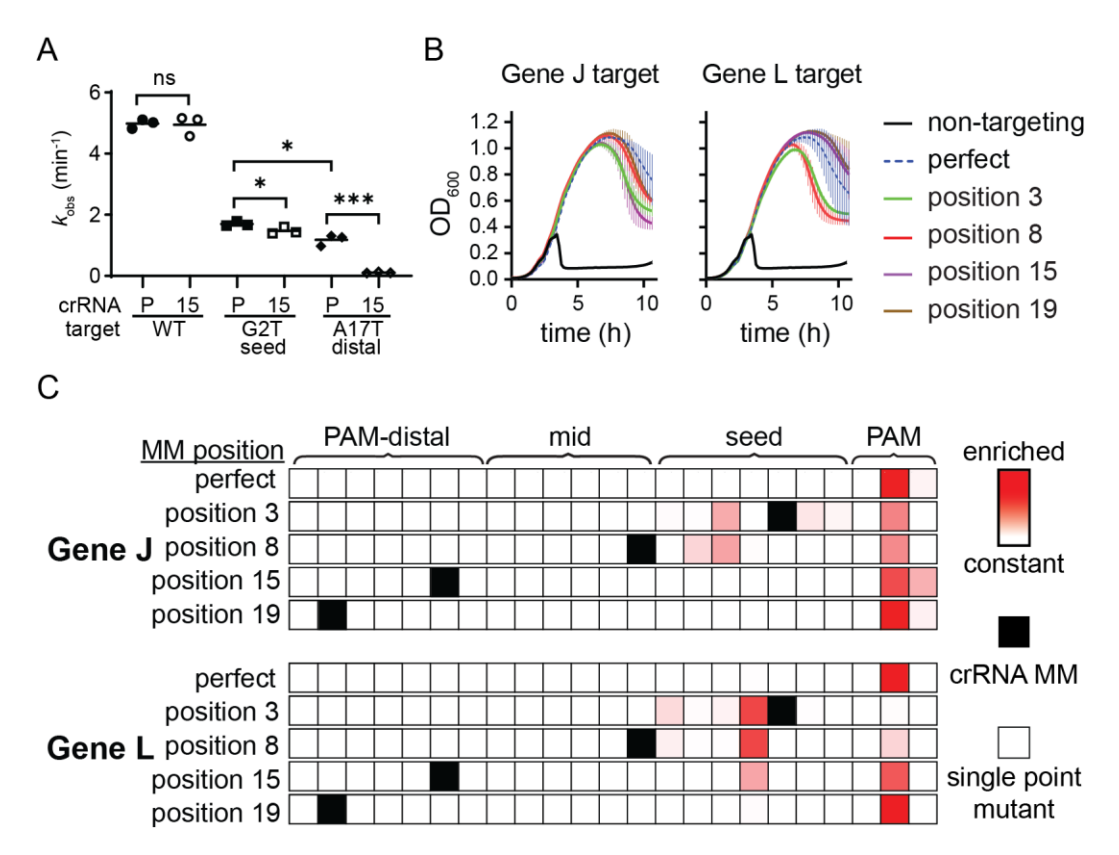


Figure 4 – Cas9 challenge does not cause emergence of PAM-distal mutants

(A) Observed rate constants for cleavage of a target plasmid bearing a wild type (WT), seed mutant (G2T) and PAM-distal mutant (A17T) gene L target sequence. Cas9 cleavage was measured for both the perfectly matched crRNA (P) or the MM15 crRNA (15). Significance was tested pairwise for all crRNA/target combination by unpaired two-tailed t-test. * $P \le 0.05$, *** $P \le 0.001$, ns P > 0.05. Pairwise comparisons for which P value are not indicated had a P < 0.0001. See S9 Fig. for crRNA and target sequences, gels, and fit data.

(B) Growth curves of E. coli expressing Cas9 and sgRNAs bearing either a non-targeting sequence, the perfectly matching spacer sequence (perfect), or a spacer containing mismatch at the indicated position with respect to the PAM. Phage was added when the cells reached mid log phase at \sim 2 hours after inoculation. The average of three replicates is plotted for each condition, with error bars representing standard deviation.

(C) Heat maps showing the location of enriched phage mutations in target regions at the 8 h time point for gene J or L targets after Cas9-mediated selection. Z-scores for abundance of single-nucleotide variants, including nucleotide identity changes or deletions, were determined for each

- sample relative to the non-targeted control phage population. Enriched sequences indicate high
- Z-scores. Z-scores range from 0 (white) to 7.0 (darkest red).

1080

1081

1082

1083

1084

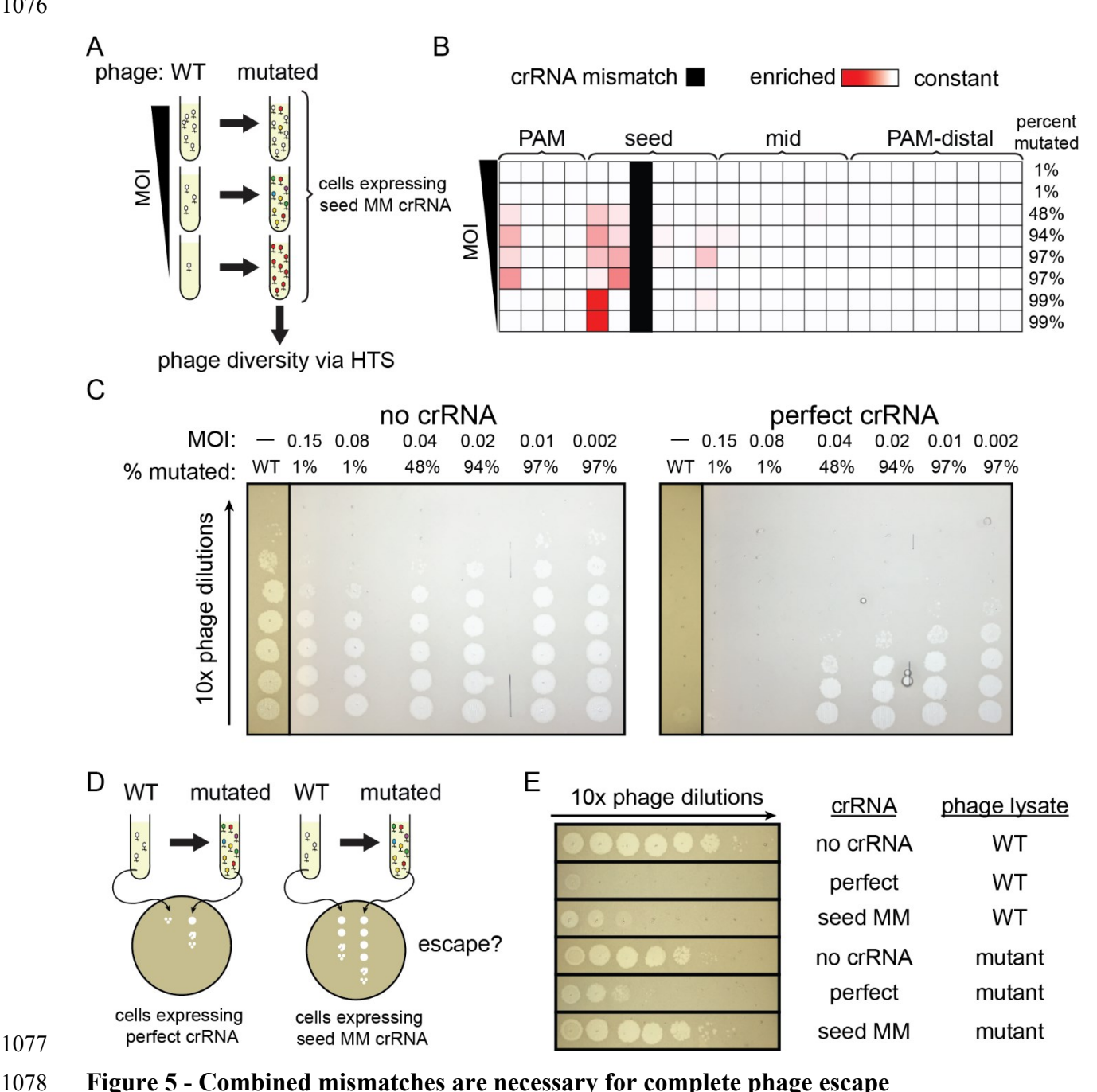


Figure 5 - Combined mismatches are necessary for complete phage escape

(A) Schematic for experiment to test the impact of MOI on escape phage diversity. Cultures expressing Cas 12a and the position 3 mismatched crRNA targeting gene J were infected with lambda phage at varied MOIs. Mutant phages in lysates were detected by high-throughput sequencing.

(B) Heat map showing the position of phage mutations that arose when infecting bacteria expressing seed mismatch crRNA at different MOIs. Phage was harvested from liquid cultures

1085 containing bacteria expressing FnCas12a and a crRNA with a C-T mismatch at position 3. Phage 1086 was added to the culture at mid-log phase at a range of MOIs starting at 0.15 and serial 2-fold dilutions from 1/2 to 1/32 and an additional sample at an MOI of 1.5 x 10⁻³. Phage was harvested 1087 5 hours after infection. High-throughput sequencing was used to determine the percent of phages 1088 1089 in each that had a mutation in the target region. The heat map shows the positions in the target 1090 that were enriched with mutations. These positions are colored darker red according to their Z-1091 score relative to the control phage population. Z-scores range from 0 (white) to 10.1 (darkest red). The position of the initial crRNA mismatch is indicated in solid black 1092 (C) Spot assays using phage isolated from liquid cultures as described in (A) on bacteria 1093 1094 expressing a matching crRNA. Phage harvested in (A) was 10-fold serial diluted and spotted on 1095 bacteria with a crRNA matching the wild-type lambda phage genome target (matching crRNA) 1096 or bacteria without a crRNA guiding Cas12a (no crRNA). Wild-type phage controls were spotted 1097 on these same bacterial strains. Phages harvested from the lowest MOI cultures were omitted due 1098 to their low titer which prevented visible plaque formation on the CRISPR active E. coli strain. 1099 See S11b Fig. for full plates. 1100 (D) Schematic for experiment shown in panel (E). Wild-type or mutant phage populations were used for spot assays on plates with lawns of E. coli expressing Cas 12a and either the perfect or 1101 1102 the seed mismatched crRNA to determine whether the combination of the pre-existing mismatch 1103 and newly acquired target mutations are necessary for complete escape from Cas12a targeting. 1104 (E) Spot assays using mutationally diverse phage on bacteria expressing crRNAs with and 1105 without mismatches. Phage was isolated from the liquid culture as described in (A) that was 1106 initially infected with phage diluted 1:8. Mutated phage and unmutated control phage (WT) were 1107 then used for spot assays on bacterial lawns expressing FnCas12a and a matching crRNA 1108 (perfect), a crRNA with the original seed mismatch, or no crRNA as negative control.

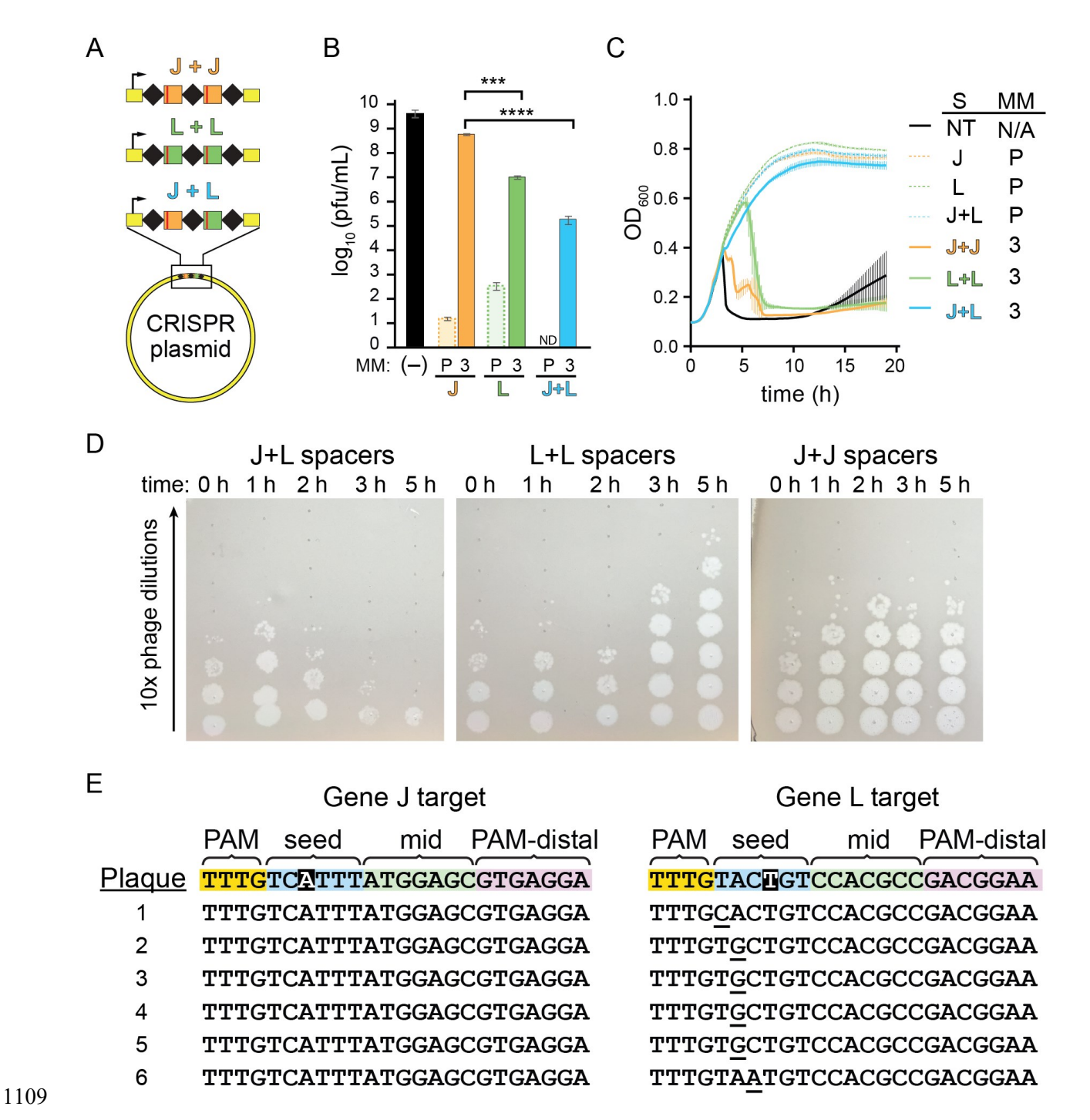
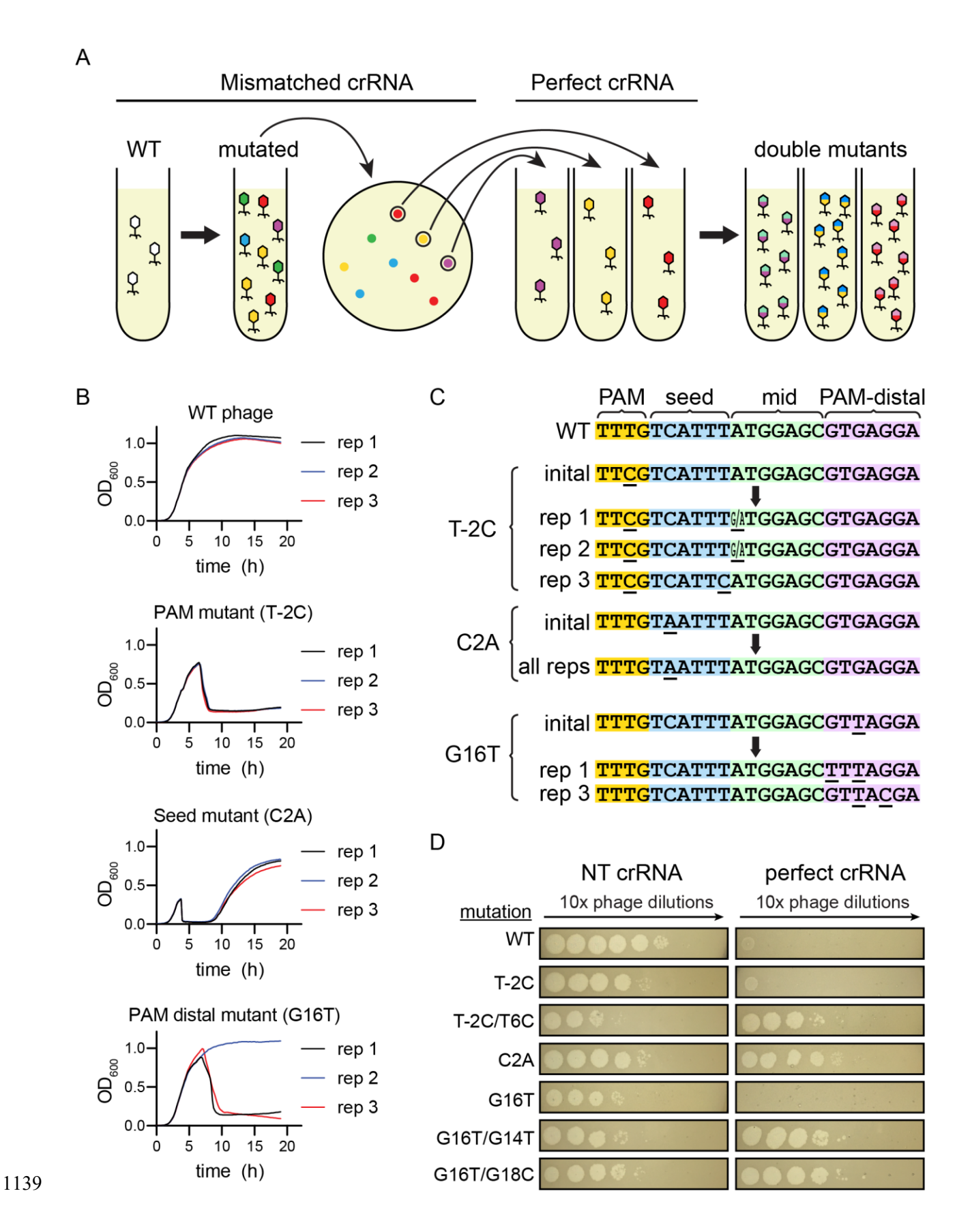


Figure 6 - Multiple mismatched crRNAs provide more protection than individual mismatched crRNAs

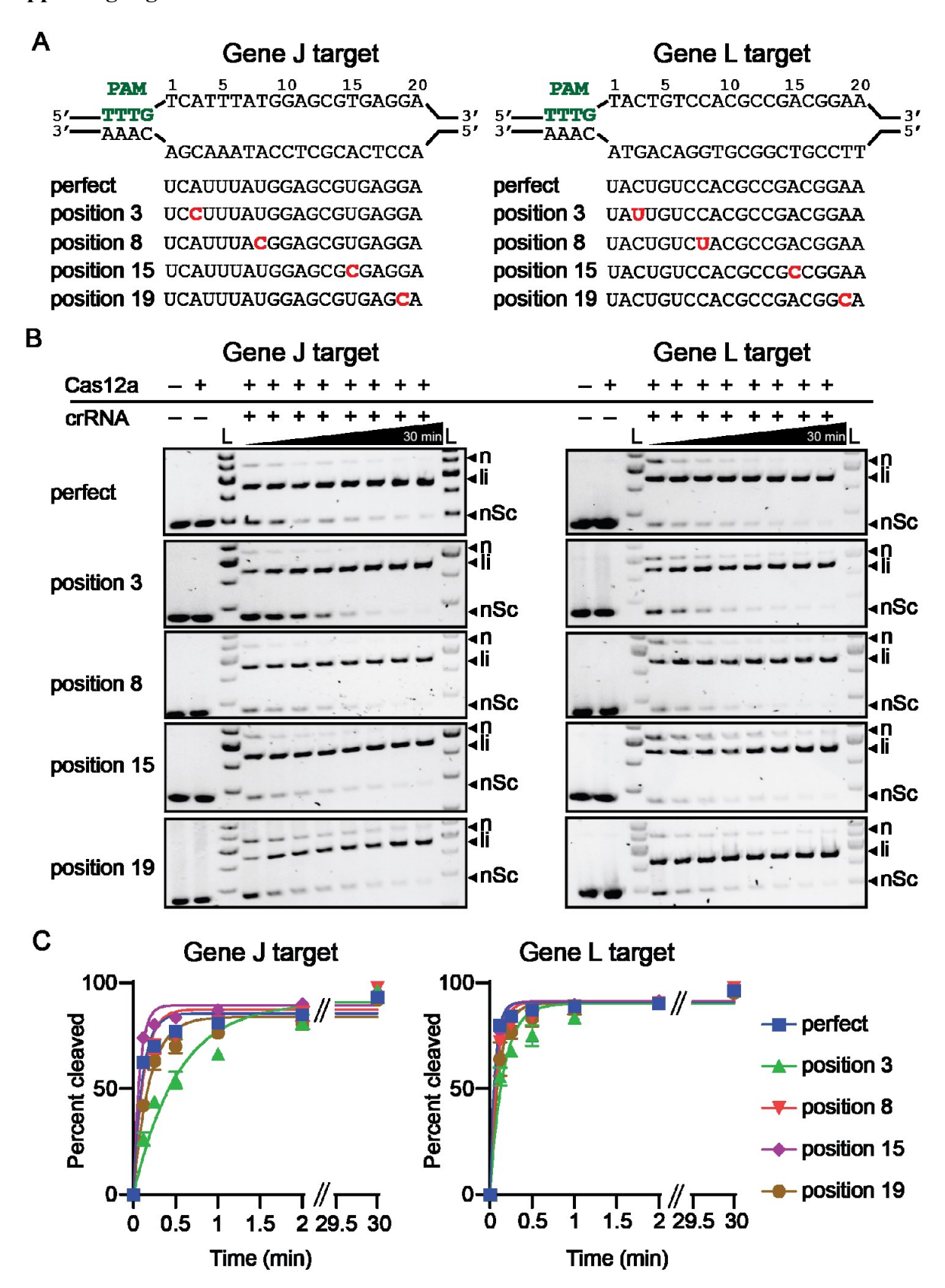
(A) Schematic of experiment in which two crRNAs bearing mismatches at position 3 are expressed from a CRISPR plasmid. The CRISPRs either have two identical spacers targeting gene J (J+J) or gene L (L+L), or have two different spacers targeting gene J and L (J+L).

- (B) Number of plaques formed on lawns of bacteria expressing multiple mismatched crRNAs.
- Plaque assays were performed using bacteria containing a plasmid expressing FnCas12a along
- with different crRNA expression plasmids. Plasmid expressed either the perfect crRNA (P) or
- the position 3 mismatched crRNA (3). For the perfect crRNAs, plasmids expressed either one
- 1119 (gene J or gene L alone) or two (J+L) spacers. For the position 3 mismatched crRNAs, each
- 1120 crRNA expression plasmid contains two spacers: both targeting gene J both targeting gene L and
- one spacer targeting each of gene J and gene L (J+L). (-) indicates a negative control in which no
- 1122 crRNA was expressed. Plaque forming units (pfu) was calculated using the number of plaques on
- each plate and the volume of phage lysate added. The average of multiple replicates (n = 2 to 4)
- is plotted with error bars representing standard deviation. Unpaired, two-tailed t-tests were used
- to determine the statistical significance of each of the single spacer constructs compared to the
- double spacer construct, *** $P \le 0.001$, **** $P \le 0.0001$.
- 1127 (C) Growth curves using the same bacterial strains described in (A). Phage was added when the
- cells reached mid log phase at ~2 hours after inoculation. The average of three replicates is
- plotted for each condition, with error bars representing standard deviation.
- (D) Spot assays used to measure the titer of phage over time in phage infection cultures. Spot
- assays were performed using 10-fold serial dilutions of phage harvested from cultures in (B) that
- infected bacterial strains with two mismatched spacers at different time points on lawns of
- 1133 CRISPR-inactive *E. coli*.
- 1134 (E) Sequences of both CRISPR targets in single phage plaques for phage harvested from E. coli
- cultures expressing a double spacer construct. The two crRNAs contained mismatches at
- positions highlighted in black. Target regions for the gene J and gene L target were sequenced
- for six individual plaques using Sanger sequencing. Target sequences are aligned to the WT
- sequence (top row) and mutations are underlined. See S12b Fig. for chromatograms.



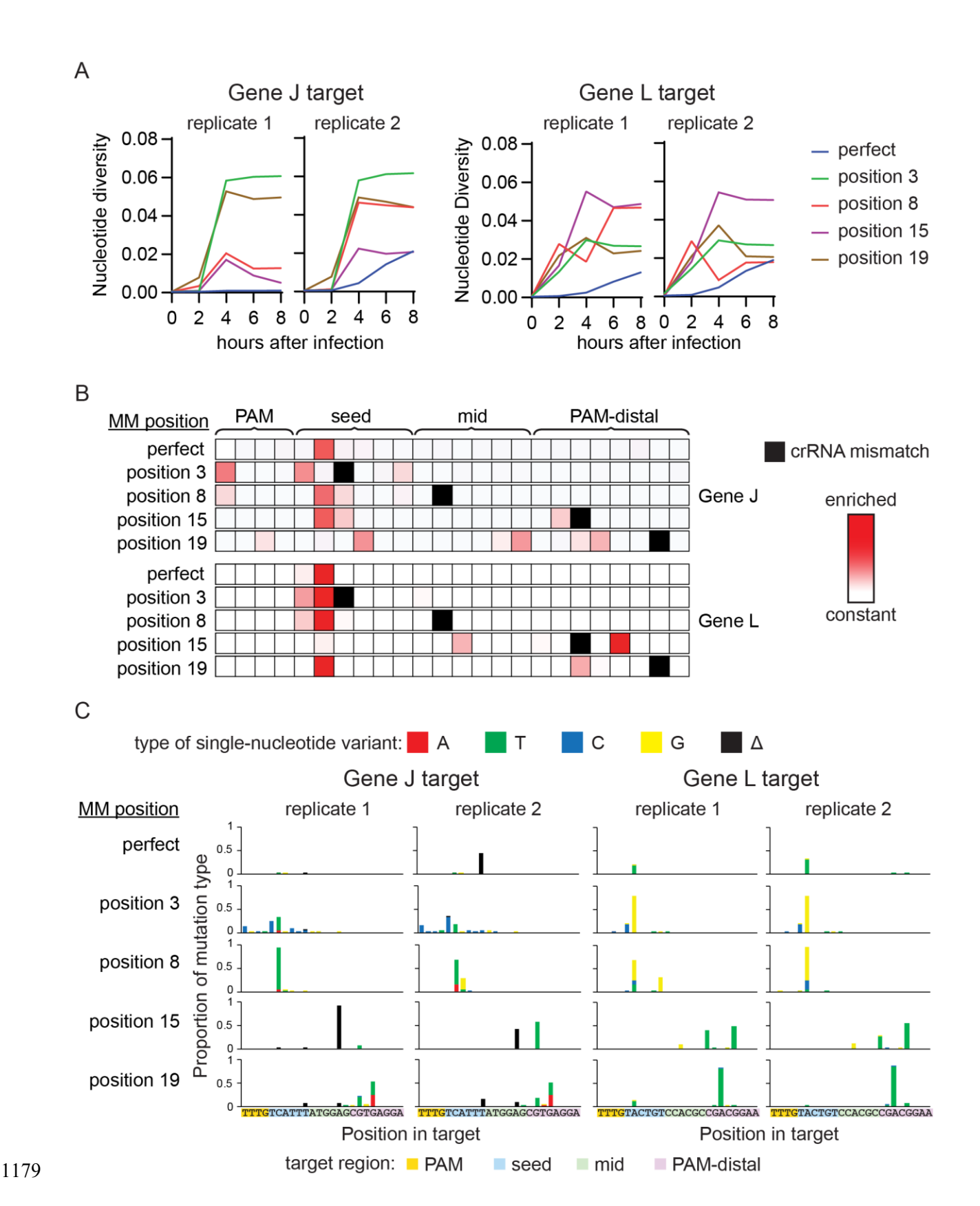
1140 Figure 7 - Generation of double mutant phage is driven by insufficiently deleterious 1141 mutations 1142 (A) Schematic of the process for generating and purifying single mutant phage populations. 1143 Wild-type phage was used to challenge E. coli expressing a crRNA with a mismatch to the target in the phage genome in liquid culture. The resulting phage were isolated and used for a plaque 1144 assay on lawns of bacteria expressing the same mismatched crRNA. Single plaques were isolated 1145 1146 and again used to challenge bacteria expressing a mismatched crRNA in liquid culture, further 1147 purifying and propagating single mutants. Finally, single mutant phages were used to challenge 1148 bacteria expressing a perfectly matching crRNA in liquid culture to determine whether second 1149 mutations would appear. (B) Growth curves of bacteria expressing a perfectly matching crRNA challenged with wild type 1150 1151 phage and phage with various single target mutations. Locations of the single mutations in the 1152 target are labeled (PAM mutant, Seed mutant, and PAM distal mutant). Position and type of 1153 mutations are indicated in parenthesis. Three biological replicates are shown separately for each 1154 experimental condition. 1155 (C) Diagram of initial and selected mutations that appeared when a single mutant phage was 1156 used to challenge bacteria expressing a perfectly matching crRNA. Initial mutants are single 1157 mutants that were generated and purified as described in (A). Sequences below arrows show 1158 phage mutants that appeared in different biological replicates (rep 1, 2 or 3) after initial mutant 1159 phage lysates were used to infect bacteria expressing a perfectly matching crRNA in liquid culture. Positions with ambiguous base calls are indicated with two bases (X/Y) at that position. 1160 Target sequences were interpreted from Sanger sequencing chromatograms (see S13 Fig.). 1161 1162 (D) Spot assays challenging bacteria expressing a perfectly matching crRNA with various single 1163 and double mutant phage lysates. WT phage or phages with the indicated target mutations were 1164 spotted on bacteria expressing a non-targeting crRNA (left column) and a perfectly matching 1165 crRNA (right column).

Supporting Figures



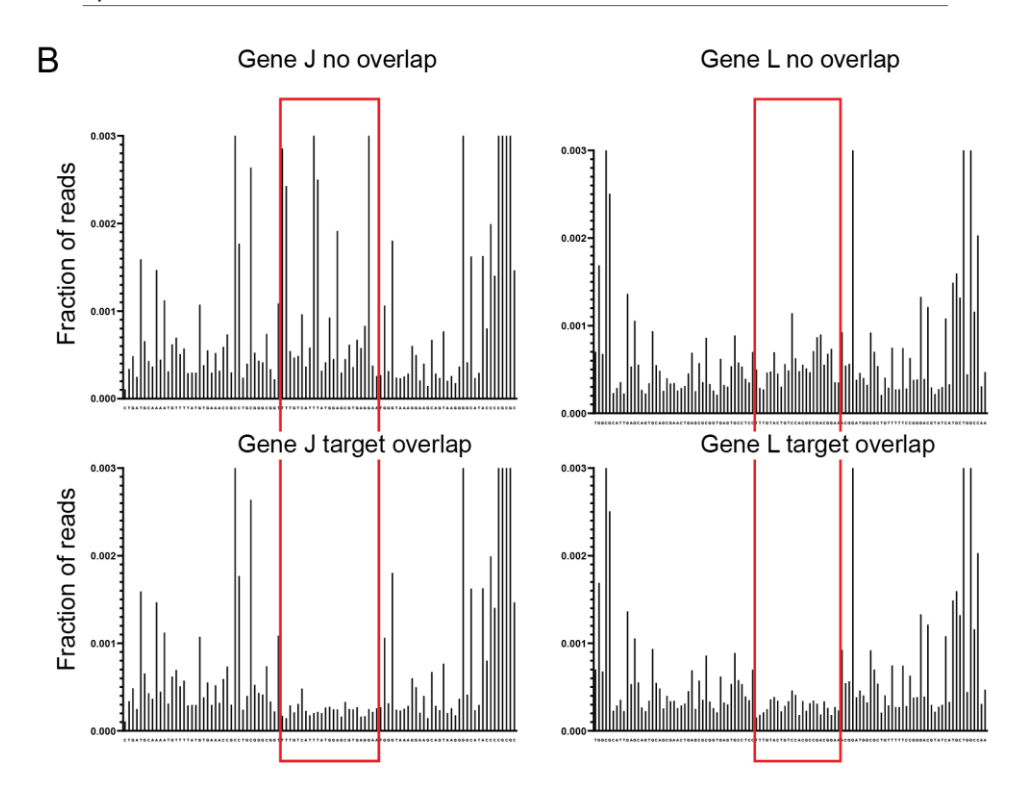
1168	S1 Figure - Cleavage assays by FnCas12a with single mismatch crRNAs
1169	(A) Sequence of the target DNAs, perfectly matching crRNAs and single-mismatched crRNAs.
1170	(B) Representative agarose gels showing time course cleavage of negatively supercoiled plasmid
1171	(nSC) using perfectly matching crRNA or single-mismatched crRNA by FnCas12a, resulting in
1172	linear (li) and/or nicked (n) products. Time points at which the samples were collected were 7 s,
1173	15 s, 30 s, 1 min, 2 min, 5 min, 15 min, and 30 min. All controls were performed under the same
1174	conditions as the longest time point for the experimental samples.
1175	(C) Quantification of cleaved products (linear and nicked fractions) from the time course
1176	cleavage. Averages of the cleaved fraction values were plotted versus time and fit to a first-order
1177	rate equation with error bars; $n = 3$ replicates. For values reported in Figure 1c, each individual

replicate was fit, and $k_{\rm obs}$ was reported as the average value for the three replicates.



(A) Line graphs showing the nucleotide diversity of phage target regions over time after exposure to bacteria cells expressing crRNAs with and without mismatches. Target regions are gene J or gene L and crRNAs either match the target region (perfect) or contain mismatches at position x. Nucleotide diversity is calculated using the proportion of each sequence in the samp and the number of nucleotide differences between each pair of sequences. Two individual replicates are shown for each condition. (B) Heat maps showing location of target mutations that arose due to CRISPR targeting by FnCas12a on a solid medium. Z-scores for abundance of single-nucleotide variants, including nucleotide identity changes or deletions, were determined for each sample relative to the non-
gene J or gene L and crRNAs either match the target region (perfect) or contain mismatches at position x. Nucleotide diversity is calculated using the proportion of each sequence in the samp and the number of nucleotide differences between each pair of sequences. Two individual replicates are shown for each condition. (B) Heat maps showing location of target mutations that arose due to CRISPR targeting by FnCas12a on a solid medium. Z-scores for abundance of single-nucleotide variants, including
position x. Nucleotide diversity is calculated using the proportion of each sequence in the samp and the number of nucleotide differences between each pair of sequences. Two individual replicates are shown for each condition. (B) Heat maps showing location of target mutations that arose due to CRISPR targeting by FnCas12a on a solid medium. Z-scores for abundance of single-nucleotide variants, including
and the number of nucleotide differences between each pair of sequences. Two individual replicates are shown for each condition. (B) Heat maps showing location of target mutations that arose due to CRISPR targeting by FnCas12a on a solid medium. Z-scores for abundance of single-nucleotide variants, including
replicates are shown for each condition. (B) Heat maps showing location of target mutations that arose due to CRISPR targeting by FnCas12a on a solid medium. Z-scores for abundance of single-nucleotide variants, including
1188 (B) Heat maps showing location of target mutations that arose due to CRISPR targeting by 1189 FnCas12a on a solid medium. Z-scores for abundance of single-nucleotide variants, including
FnCas12a on a solid medium. Z-scores for abundance of single-nucleotide variants, including
nucleotide identity changes or deletions, were determined for each sample relative to the non-
targeted control phage population. Enriched sequences indicate high Z-scores. Z-scores range
from 0 (white) to 7.7 (darkest red). Single nucleotide deletions are shown at adjacent position to
the 3' side. Positions with crRNA mismatches are labeled with solid black boxes in the heat ma
1194 (C) Graphs showing single-nucleotide variations for mutated phage target sequences present at
the 8 h time point for two individual replicates. Bar graph height shows the proportion of
sequences in each sample with the mutation type at each position in the target. Deletions (Δ) are
plotted at the first position where a mismatch occurs between the crRNA and the target.

Α		Gene	J target	Gene L	target	
		number of reads			number of reads	
	<u>crRNA</u>	<u>rep 1</u>	<u>rep 2</u>	<u>rep 1</u>	<u>rep 2</u>	
	non-targeting	644959	240080	702921	627352	
	perfect	40833	47381	35357	44965	
	position 3	91218	86032	74030	68508	
	position 8	83682	82296	70347	72941	
	position 15	89176	85471	72068	66747	
	position 19	90221	75516	88252	78551	

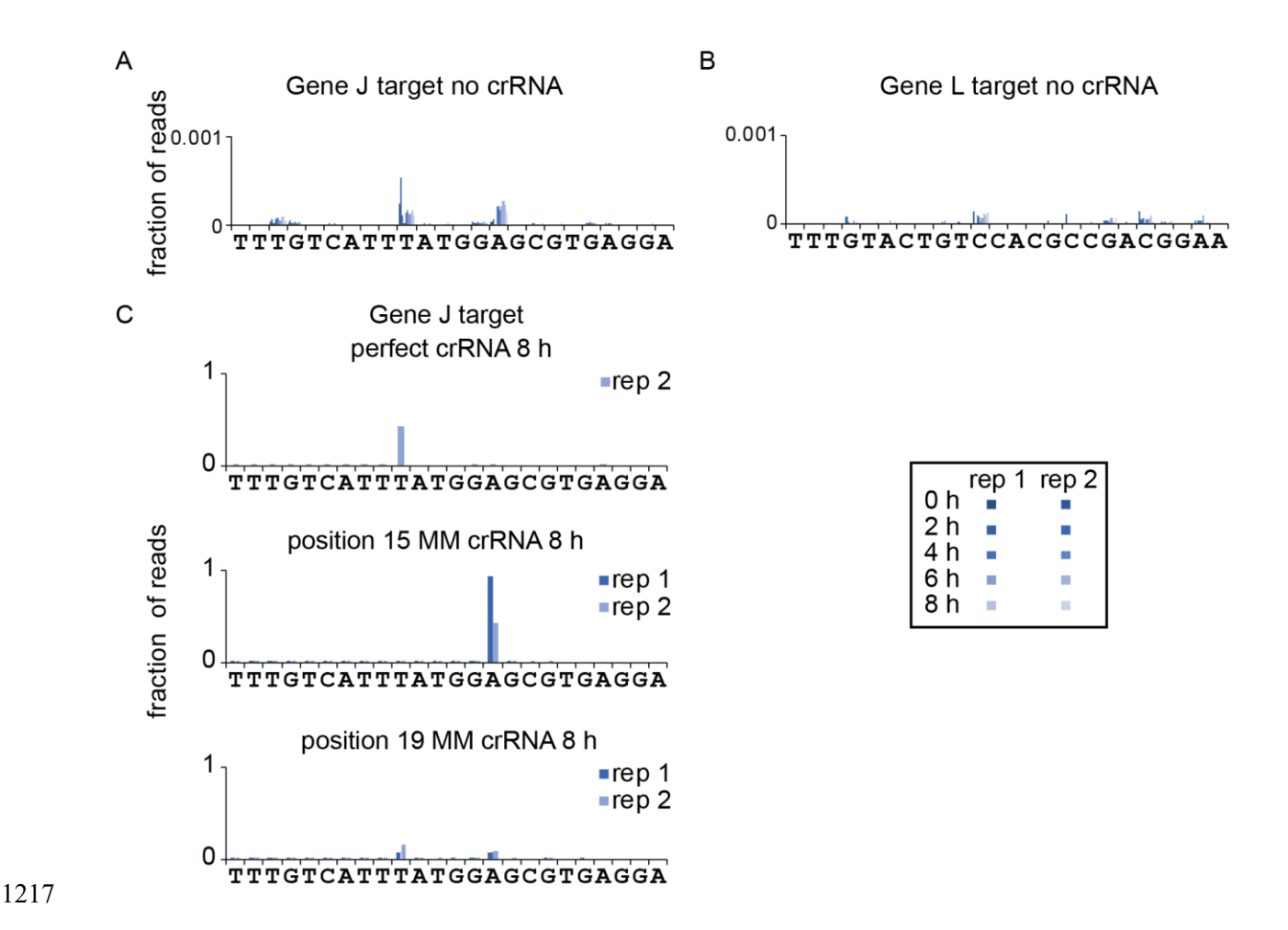


S3 Figure - MiSeq sample counts and R1/R2 file overlap

(A) Table showing absolute counts from MiSeq for each replicate of the 8 h time point for each experimental condition for *E. coli* infected with wild-type phage. Each count represents an extracted sequence in which R1 and R2 reads matched. The negative control (non-targeting crRNA) samples were run in a separate MiSeq run to maximize the number of reads and minimize barcode overlap with mutated samples, allowing for analysis of pre-existing mutants in the wild-type population.

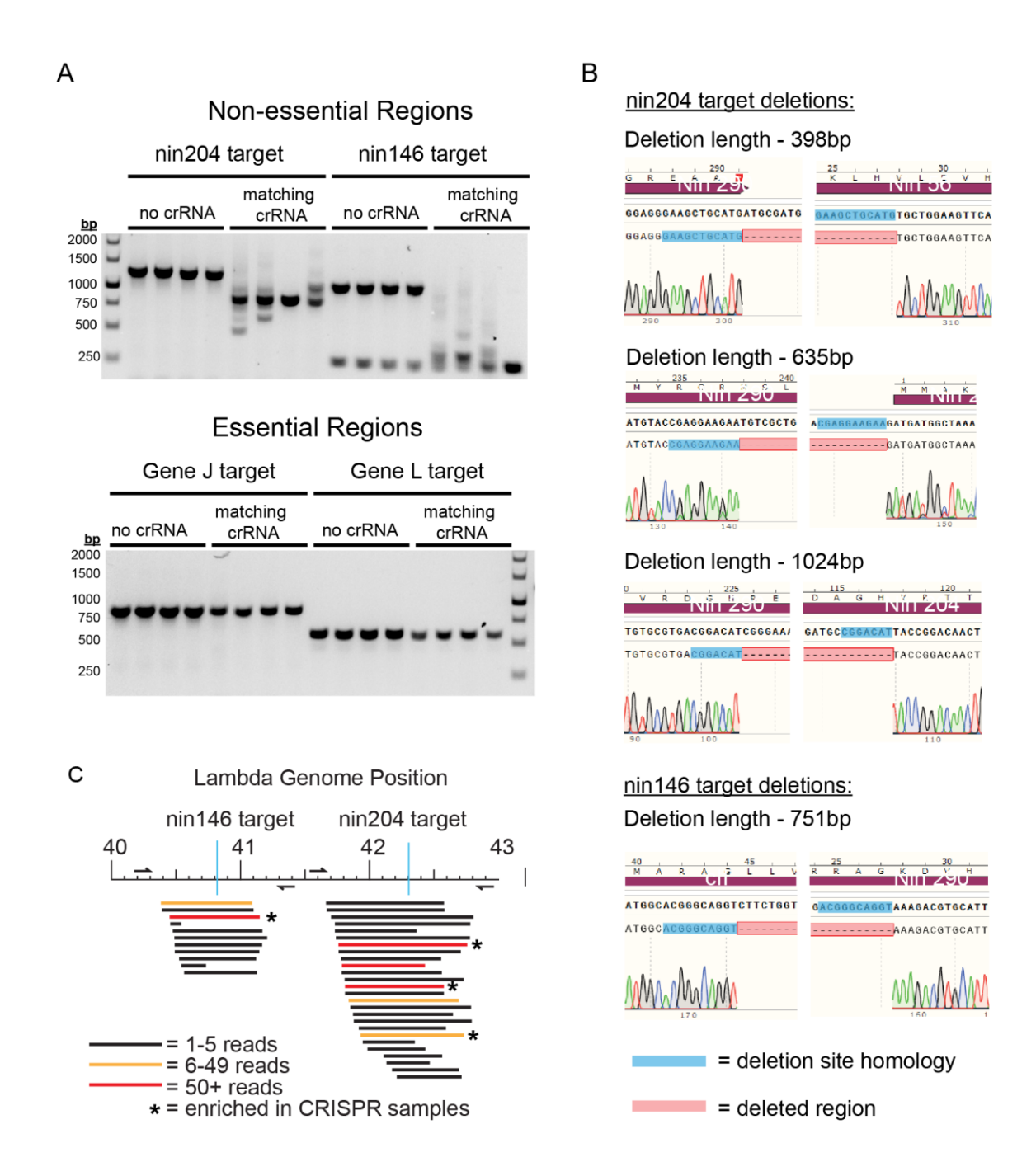
(B) Bar charts showing mutated sequences at each position in the high-throughput sequencing reads of the negative control lambda phage population for the gene J and gene L region. The target region is highlighted with a red box. R1 and R2 reads do not overlap in the target region

(no overlap) or overlap in the target region (target overlap). R1 reads are used for the target region in the no overlap condition. When R1 and R2 reads overlap, sequences in which the target region sequence does not agree for both the R1 and R2 reads are removed from analysis and are not shown in this figure. This measure was taken to ensure that variations observed in negative control samples arose solely from PCR errors or the natural variation of the population. While some variations were still observed with stringent R1/R2 overlap enforced, it is not possible to distinguish PCR errors from natural variation. No mutations were substantially enriched outside of the target region for any of the samples tested in this study.



S4 Figure - Single deletions enriched by CRISPR exposure

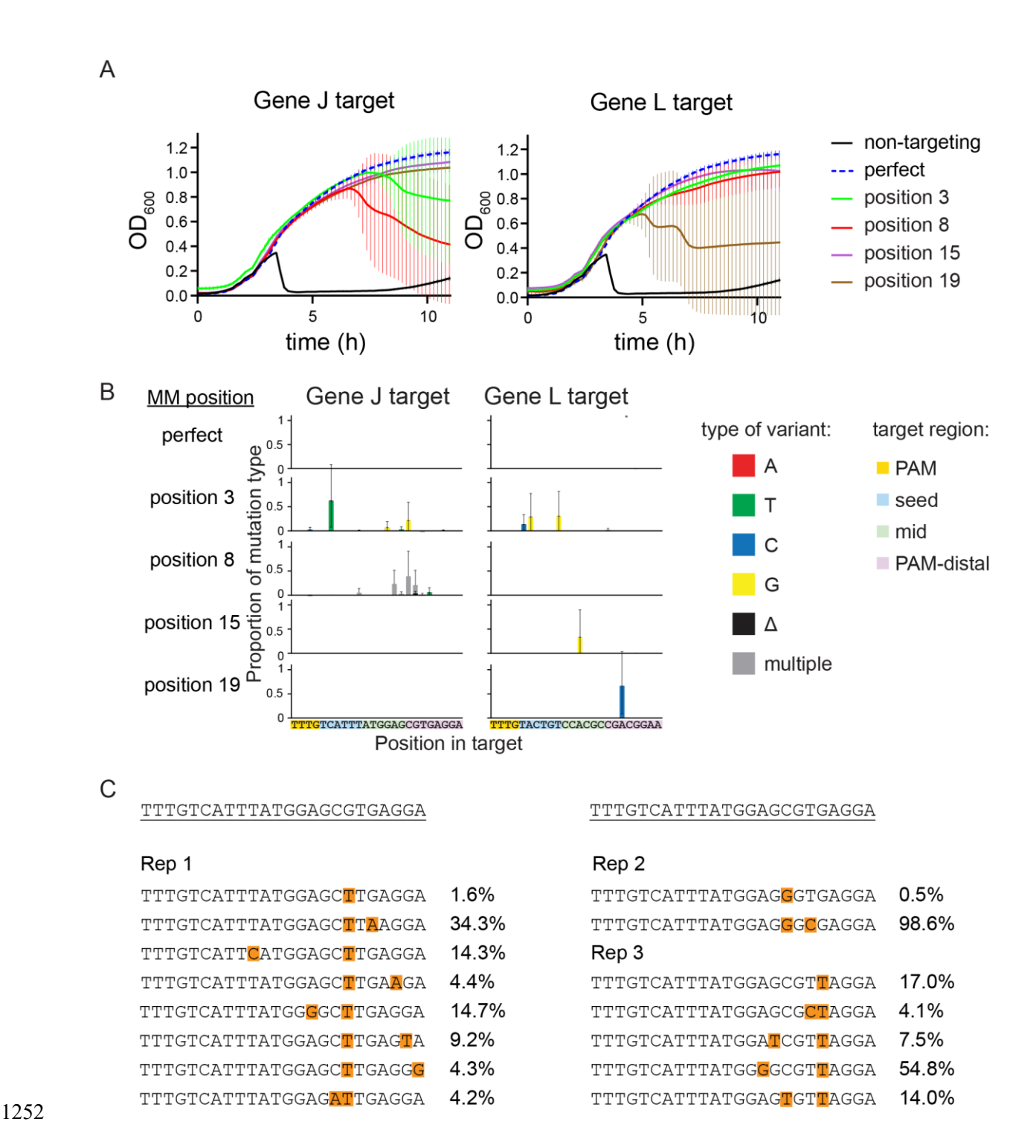
Bar charts showing single nucleotide deletions from the lambda phage gene J target (A) and gene L target (B) in phage that were exposed to cells expressing a non-targeting crRNA (CRISPR inactive) and cells expressing crRNAs with and without mismatches to the lambda phage gene J target (C). (A-B) Deletions are mapped along the target sequences for all time points and both biological replicates for the negative control samples. (C) CRISPR active samples shown for gene J target that contained deletion sequences that represented more than 1% of all reads. No such deletions were observed in the gene L target. Deletions were observed in the gene L coding region in phage in the wild-type population. The deletions could remain in genomes in the population as these genomes are packaged along with functional structural proteins in successfully infected cells.



S5 Figure - Deletions in non-essential genomic regions that are selected following Cas12a targeting pre-exist in the phage population

(A) PCR amplification of regions surrounding essential and non-essential genes targeted by Cas12a. Spot assays were performed using *E. coli* expressing crRNAs that match two non-essential (nin204 and nin146) and two essential regions (gene J and gene L) of the lambda phage genome. Controls were performed with a plasmid not encoding a crRNA. Phages were isolated

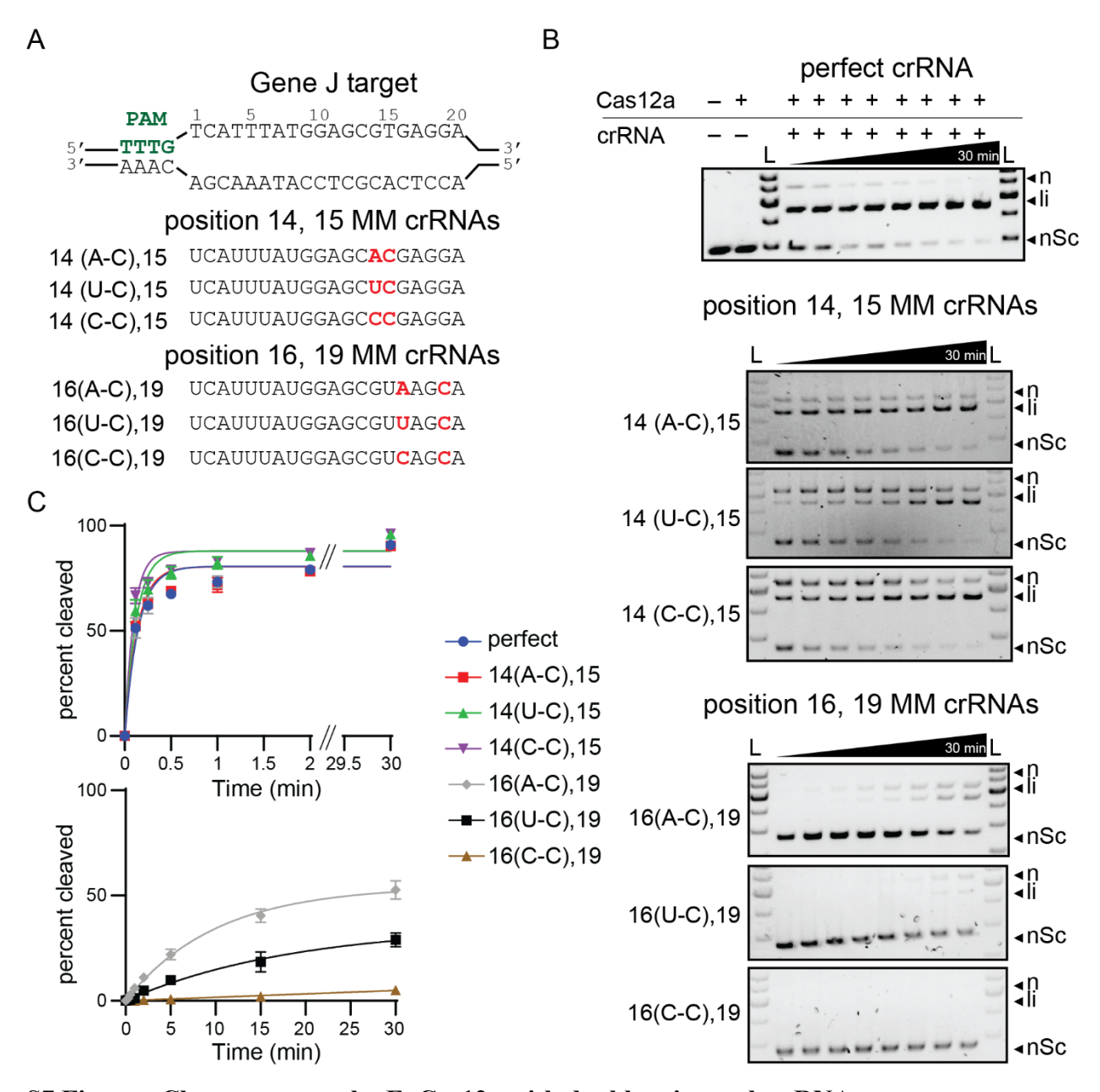
1236 from the phage spots and target and flanking regions of the phage genome were PCR amplified 1237 and run on an agarose gel. 1238 (B) Sanger sequencing chromatograms of phage genome deletions in non-essential regions 1239 targeted by Cas12a. Non-essential regions in the lambda phage genome were targeted with 1240 matching crRNAs on solid media. Phages were isolated and the target regions were PCR amplified. Single bands were gel purified and PCR amplified in a second round. These second 1241 PCR products were sequenced and the chromatograms were aligned to the WT lambda phage 1242 genome. Homology at each end of the deletions was identified and highlighted in blue. 1243 (C) Map of genomic deletions observed by PacBio sequencing of PCR amplicons from phage 1244 unexposed to CRISPR targeting. DNA from lambda phage unexposed to CRISPR targeting was 1245 used as a template for PCR reactions that amplified the same non-essential regions as in (a). This 1246 PCR product was sequenced with PacBio long-read sequencing and the obtained sequences were 1247 matched with the wild-type lambda genome sequence to identify any deletions present. These 1248 1249 deletions are plotted on the chart relative to their position in the genome. The quantity of each 1250 deletion is identified by a color code. Deletions found by Sanger sequencing in CRISPR active 1251 samples are indicated with an asterisk (*).



S6 Figure – Growth curves and mutant emergence for Δred phage infection

(A) Growth curves of *E. coli* expressing FnCas12a and crRNAs bearing non-targeting, perfectly matching, or mismatched crRNAs infected with Δred phage. Phage was added when the cells reached mid log phase at ~2 hours after inoculation. The average of three replicates is plotted for

1257 each condition, with error bars representing standard deviation. Large error bars indicate that not all replicate cultures lysed. 1258 1259 (B) Graphs showing mutation type in $\triangle red$ phage target sequences present at the 8 h time point. Bar graph height shows the proportion of sequences in each sample with the mutation type at 1260 1261 each position in the target. Deletions (Δ) and multiple mutations are plotted at the first position where a mismatch occurs between the crRNA and the target. The average of three replicates is 1262 1263 shown, with error bars representing standard deviation. (C) Comparison of target sequences of phage isolated from cultures in (A) containing cells 1264 expressing a crRNA targeting gene J with a mismatch at position 8. The WT target sequence is 1265 underlined. Three individual replicates are shown and the percent of each mutant sequence in the 1266 sample is listed. Mutated positions relative to the WT sequence are highlighted in orange. 1267

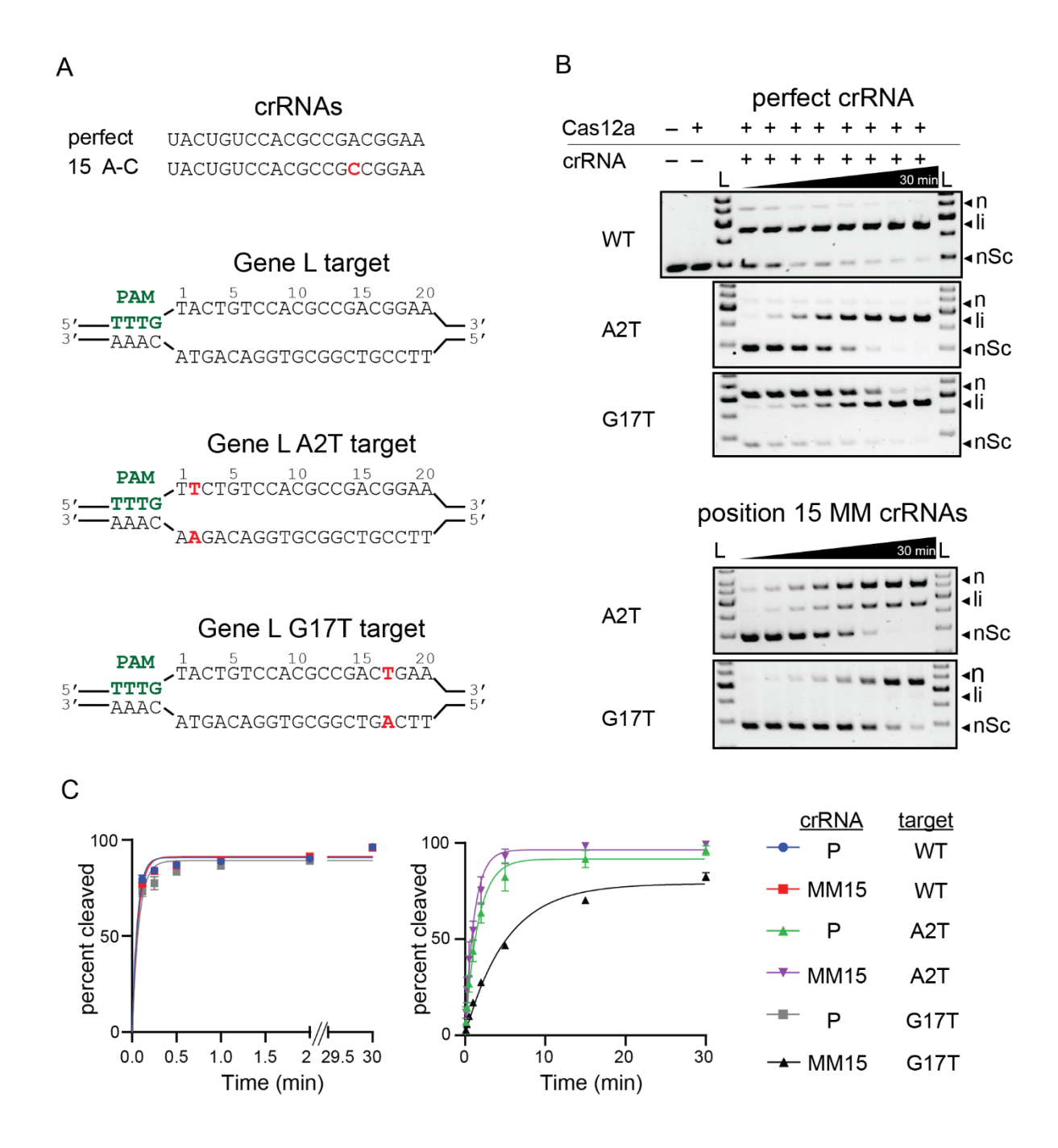


S7 Figure - Cleavage assays by FnCas12a with double mismatch crRNAs

(A) Sequence of the gene J target DNA, perfectly matching crRNA and double-mismatched crRNAs.

(B) Representative agarose gels showing time course cleavage of negatively supercoiled plasmid (nSC) using perfectly matching crRNA or double-mismatched crRNA by FnCas12a, resulting in linear (li) and/or nicked (n) products. Time points at which the samples were collected were 7 s, 15 s, 30 s, 1 min, 2 min, 5 min, 15 min, and 30 min. All controls were performed under the same conditions as the longest time point for the experimental samples.

(C) Quantification of cleaved products from the time course cleavage. The average cleaved fraction was plotted versus time and fit to a first-order rate equation with error bars representing standard deviation; n = 3 replicates. For values reported in Figure 3b, each individual replicate was fit, and $k_{\rm obs}$ was reported as the average value for the three replicates.



S8 Figure - Cleavage assays by FnCas12a of wild-type and mutant target sequences

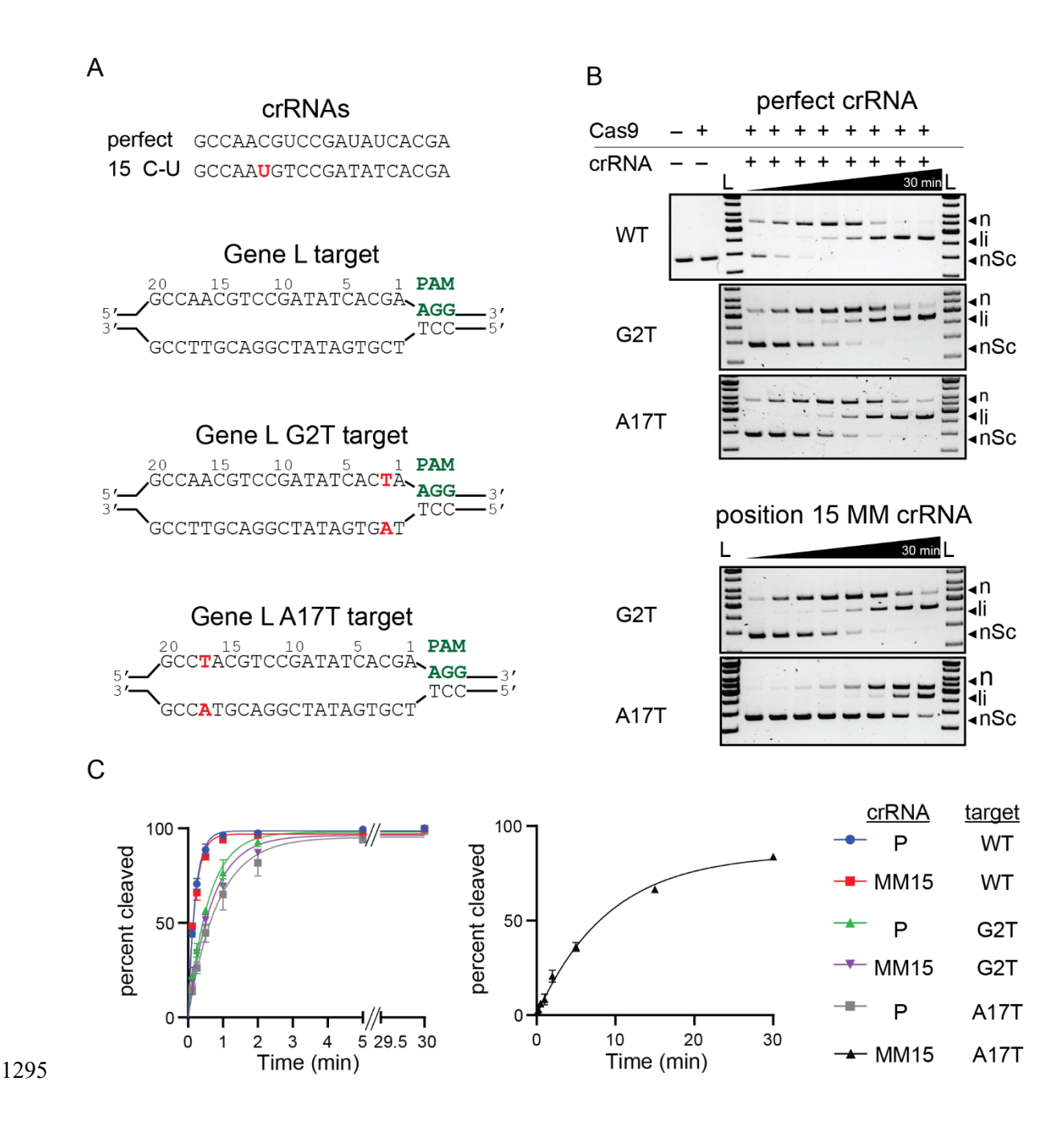
(A) Sequences the perfectly matching crRNA, position 15 mismatched crRNA, and three gene L target sequences used for cleavage assays.(B) Representative agarose gels showing time course cleavage of negatively supercoiled plasmid

matching crRNA or position 15 mismatched crRNA by FnCas12a, resulting in linear (li) and/or

(nSC) bearing a wild-type (WT), A2T, or G17T-containing gene L sequence using perfectly

nicked (n) products. Time points at which the samples were collected were 7 s, 15 s, 30 s, 1 min, 2 min, 5 min, 15 min, and 30 min. All controls were performed under the same conditions as the longest time point for the experimental samples.

(C) Quantification of cleaved products from the time course cleavage. The average cleaved fraction was plotted versus time and fit to a first-order rate equation with error bars representing standard deviation; n = 3 replicates. For values reported in Figure 3d, each individual replicate was fit, and $k_{\rm obs}$ was reported as the average value for the three replicates.



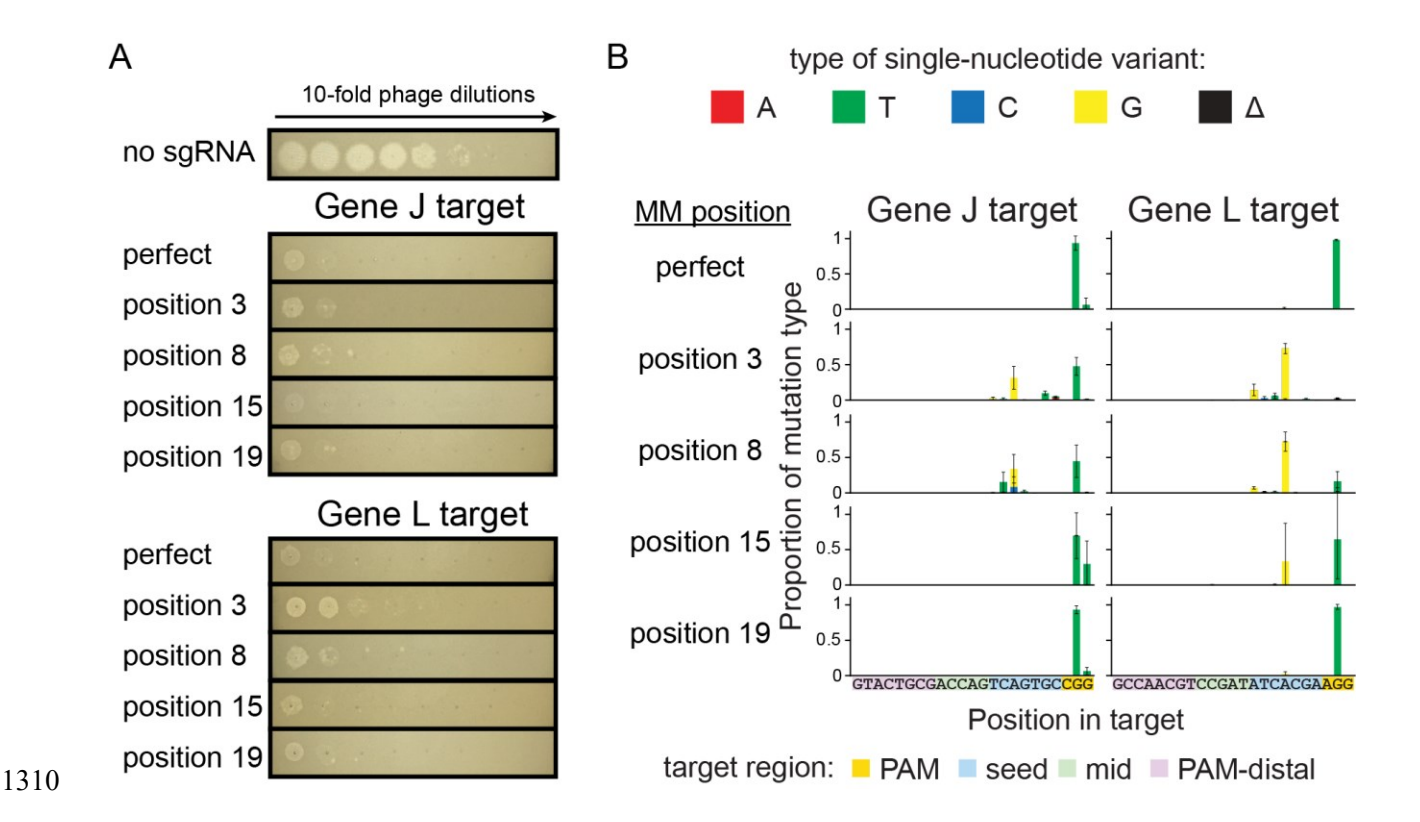
S9 Figure - Cleavage assays by SpCas9 of wild-type and mutant target sequences

(A) Sequences the perfectly matching crRNA, position 15 mismatched crRNA, and three gene L target sequences used for cleavage assays. Cleavage was performed using a crRNA-tracrRNA pair.

(B) Representative agarose gels showing time course cleavage of negatively supercoiled plasmid (nSC) bearing a wild-type (WT), G2T, or A17T-containing gene L sequence using perfectly matching crRNA or position 15 mismatched crRNA by SpCas9, resulting in linear (li) and/or

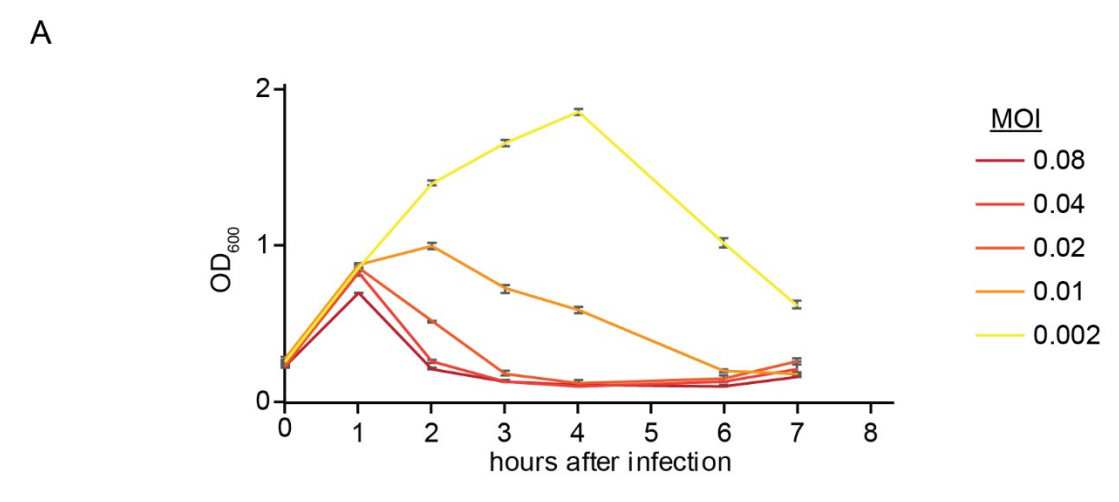
nicked (n) products. Time points at which the samples were collected were 7 s, 15 s, 30 s, 1 min, 2 min, 5 min, 15 min, and 30 min. All controls were performed under the same conditions as the longest time point for the experimental samples.

(C) Quantification of cleaved products from the time course cleavage. The average cleaved fraction was plotted versus time and fit to a first-order rate equation with error bars representing standard deviation; n = 3 replicates. For values reported in Figure 4a, each individual replicate was fit, and $k_{\rm obs}$ was reported as the average value for the three replicates.

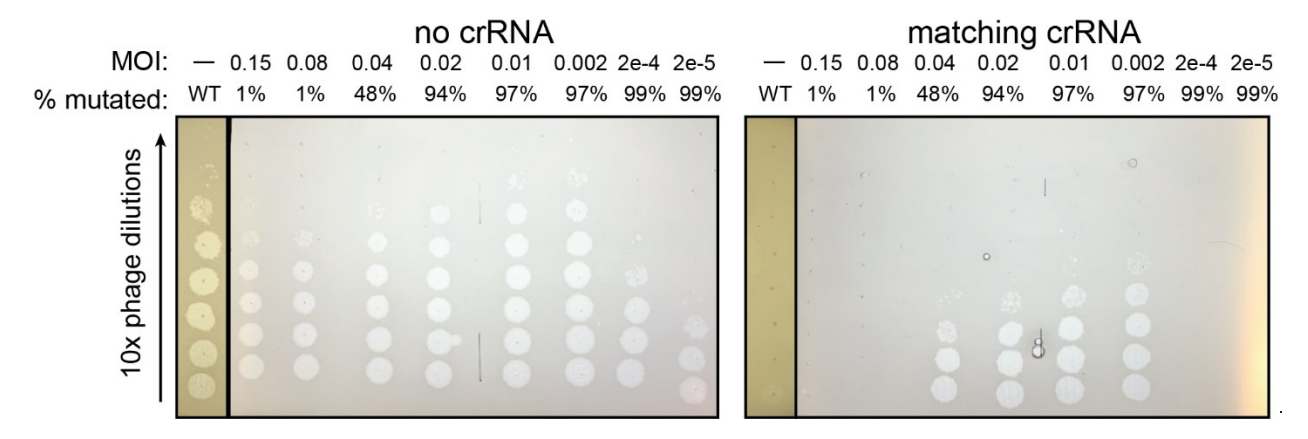


S10 Figure - Phage protection by and mutant emergence from SpCas9 with sgRNA mismatches

(A) Spot assays using lambda phage on lawns of bacteria expressing SpCas9 along with sgRNAs with and without mismatches. SgRNAs target gene J or gene L and contain mismatches at position X or match the target (perfect).
(B) Graphs showing single nucleotide variants in phage target sequences present at the 8 h time point following challenge by Cas9 bearing different sgRNAs. Bar graph height shows the proportion of sequences in each sample with the mutation type at each position in the target.
Deletions (Δ) are plotted at the first position where a mismatch occurs between the crRNA and the target. The average of three replicates is shown, with error bars representing standard deviation.



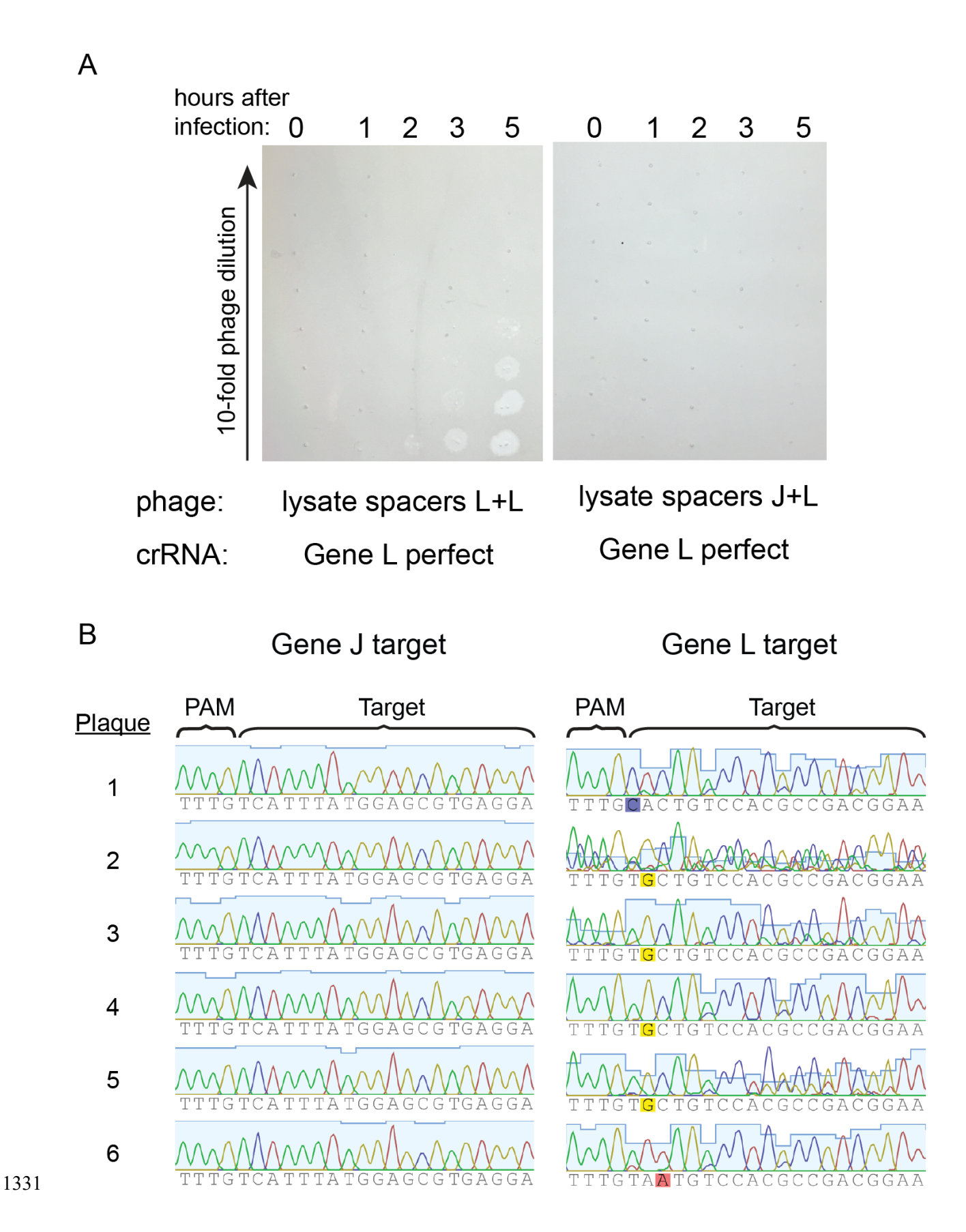
В



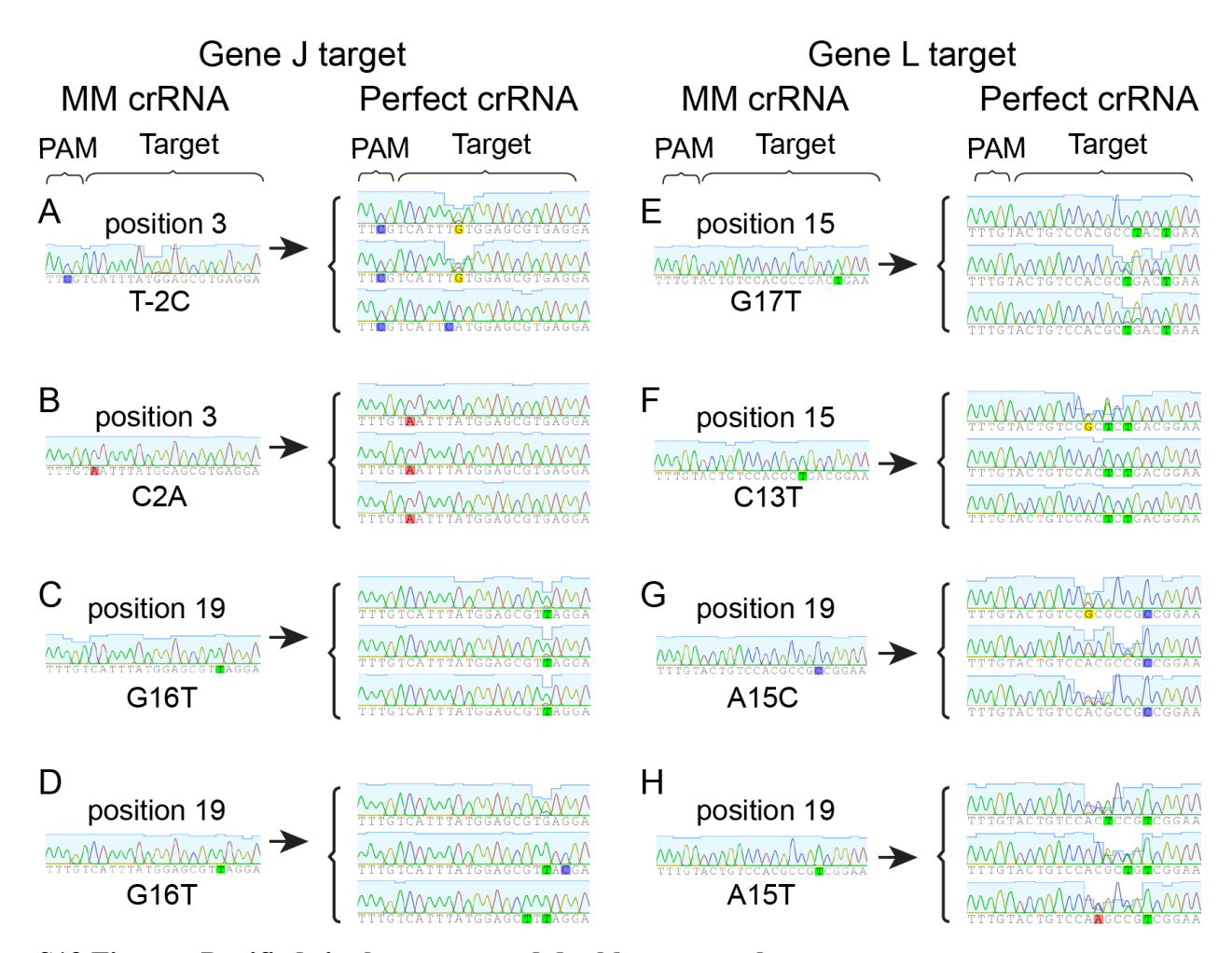
S11 Figure - Mutant emergence at varied MOIs

(A) Growth curves using cells expressing a crRNA targeting gene J with a mismatch in the seed region and infected with phage at different MOIs. Phage was added at the indicated MOIs when cells reached mid log phase and the OD_{600} of the culture was measured over time. Cultures at lower MOIs did not lyse and are omitted from the graph.

(B) Spot assays estimating the titer of phage lysates exposed to interference by Cas12a armed with a seed mismatched crRNA. Full plates from Fig. 4b, including lowest MOI samples which produced phages with low titers.



1332	S12 Figure - Phage targeted by multiple spacers develop mutations in one or more targeted
1333	regions
1334	(A) Spot assays performed using lambda phage that previously infected E. coli in liquid culture
1335	expressing FnCas12a and two different crRNAs targeting gene J and L (lysate spacers J+L) or
1336	two of the same crRNA targeting gene L (lysate spacers L+L) both with mismatches in the seed
1337	region. Phage was harvested at different time points of the liquid culture (0,1,2,3 and 5 hours
1338	after infection). The previous phage lysates were spotted on cells expressing a crRNA that
1339	matches the gene L target in the lambda genome (gene L perfect)
1340	(B) Sanger sequencing chromatograms showing sequences of target regions of the genome in
1341	phage exposed to cells expressing two mismatched crRNAs targeting gene J and gene L
1342	respectively. Phage from single plaques were isolated and both target regions were sequenced.
1343	Mutated bases are highlighted.



S13 Figure - Purified single mutant and double mutant chromatograms

(A-H) Sanger sequencing chromatograms of single and double mutant phage lysates. Single mutant phages were generated by exposure to crRNAs with mismatches (MM crRNA) at different positions (position X) and purified as shown in Fig. 7a. Mutants were generated in the gene J and gene L CRISPR target. Purified single mutant phage were used to challenge bacteria expressing a perfect crRNA and target regions were sequenced by Sanger sequencing to determine if second mutations appeared. Both mixed and clonal double mutant populations were generated after this step. Mutated bases are highlighted.

S1 Table – Lists of plasmids, primers and oligonucleotides used in this study